Quaternary Science Reviews 30 (2011) 3–27

Contents lists available at ScienceDirect

Quaternary Science Reviews

journal homepage: www.elsevier.com/locate/quascirev

Invited Review

# Contributions and unrealized potential contributions of cosmogenic-nuclide exposure dating to glacier chronology, 1990–2010

Greg Balco*

*Berkeley Geochronology Center, 2455 Ridge Road, Berkeley, CA 94709, USA*

ARTICLE INFO

*Article history:*
Received 26 August 2010
Received in revised form
2 November 2010
Accepted 3 November 2010

ABSTRACT

This paper reviews the application of cosmogenic-nuclide exposure dating to glacier chronology. Exposure dating of glacial landforms has made an outsize impact on this field because the technique filled an obvious need that had already been recognized by glacial geologists. By now, hundreds of studies have used cosmogenic-nuclide exposure dating to date glacial deposits, and in fact it is rare to find a study of glacial geology or glacier chronology, or any paleoclimate synthesis that makes use of such studies, that does not involve exposure dating. These developments have resulted in major contributions to glacier chronology and paleoclimate, in particular i) reconstructing Antarctic ice sheet change, ii) establishing the chronology of late Pleistocene and Holocene glacier change in mountain regions where it was previously unknown; iii) establishing the broad chronological outlines of mountain glaciations prior to the Last Glacial Maximum; and iv) gaining insight into subglacial erosional processes through the observation that many glaciated surfaces preserve cosmogenic-nuclide inventories from long past ice-free periods as well as the present one. An important potential future contribution will be the application of the large data set of exposure-dated glacier chronologies to better understand global and regional climate dynamics during Lateglacial and Holocene millennial-scale climate changes. However, this contribution cannot be realized without significant progress in two areas: i) understanding and accounting for geologic processes that cause apparent exposure ages on glacial landforms to differ from the true age of the landform, and ii) minimizing systematic uncertainties in exposure ages that stem from cosmogenic-nuclide production-rate estimates and scaling schemes. At present there exists an enormous data set of exposure ages on glacial deposits, but these data cannot be used to their full potential in paleoclimate syntheses due to an inadequate understanding of geologic scatter and production-rate uncertainties. The intent of this paper is to highlight this situation and suggest some strategies for realizing this potential.



## 1. Introduction

This paper reviews the application of cosmogenic-nuclide geochemistry to glacier chronology. The technology for measurement of trace cosmic-ray-produced nuclides at the concentrations present in terrestrial surface rocks developed in the late 1980s, and it became immediately obvious to glacial geologists and geochronologists that this method would be extraordinarily useful for determining the age of glacial deposits that could not be dated by any other method. By now, hundreds of studies have used cosmogenic-nuclide exposure dating to date glacial deposits, and in fact it is rare to find a study of glacial geology or glacier chronology, or any paleoclimate synthesis that makes use of such studies, that does not involve exposure dating. This paper will focus on how steady improvements in exposure-dating methods – specifically an increase in measurement precision, an increase in the number of samples that can be analysed in any one study, and the collection of more and more information about cosmogenic-nuclide production rates – have both expanded the range of questions that can be addressed with this technique and exposed new difficulties that make it harder to provide satisfying answers to these questions. At present we have available an enormous data set of exposure ages on glacial deposits. However, we are not able to use these data to their full potential in paleoclimate syntheses for lack of knowledge of, or lack of effective strategies to deal with, several important aspects of both geomorphology and cosmogenic-nuclide production. The intent of this paper is to highlight where we can make these improvements and to suggest some strategies for doing so.

* Tel.: +1 510 644 9200; fax: +1 510 644 9201.
*E-mail address:* balcs@bgc.org.

0277-3791/$ – see front matter © 2010 Elsevier Ltd. All rights reserved.
doi:10.1016/j.quascirev.2010.11.003

## 2. Basic concepts of cosmogenic-nuclide dating and application to glacial environments

### 2.1. Three basic concepts of exposure dating

This section reviews basic aspects of cosmogenic-nuclide production that are relevant to the main points of this paper, but makes no attempt to be comprehensive and omits many details of production processes that are not relevant to these points. Comprehensive reviews appear in Gosse and Phillips (2001), Balco et al. (2008), and Dunai (2010).

Three main points are important here. First, cosmogenic nuclides are rare nuclides produced in surface rocks by cosmic-ray bombardment at a rate which varies with location on the Earth's surface, but is approximately constant over time. The geographic variation of cosmogenic-nuclide production rates reflects primarily altitude – because of the shielding effect of the atmosphere, production rates are higher at higher elevations – and secondarily position in the Earth's magnetic field, which can be approximately represented by the geomagnetic latitude. Lal (1991), Stone (2000), Masarik et al. (2001), Dunai (2001), Desilets et al. (2006), and Lifton et al., (2008) have developed production-rate scaling algorithms that account for this variation, henceforth referred to as 'scaling schemes', that are broadly similar but differ in some significant details. Although the extraterrestrial cosmic-ray flux is for practical purposes invariant over the time periods relevant here, changes in the Earth's magnetic field over geological time scales do to some extent affect production rates at the Earth's surface, and some of these scaling schemes account for this variation.

The second important point is that the cosmic-ray flux, and hence cosmogenic-nuclide production, rapidly decreases with depth below the surface. Nearly all production of the cosmogenic nuclides relevant for this paper is by spallation reactions. These are reactions, between primary or secondary cosmic-ray neutrons and target elements present in surface materials, that are energetic enough to fragment the target nucleus. Spallogenic production decreases with depth below the surface according to the exponential relation

$$P_i = P_i(0)e^{\frac{-z}{\Lambda}} \quad (1)$$

where $z$ is mass depth below the surface (mass depth has units of g cm$^{-2}$ and is the product of linear depth in cm and material density in g cm$^{-3}$), $P_i$ is the production rate (atoms g$^{-1}$ yr$^{-1}$) of nuclide $i$ due to spallation at depth $z$, $P_i(0)$ is the surface production rate due to spallation, and $\Lambda$ is an effective attenuation length for spallogenic production (generally taken to be 160 g cm$^{-2}$; see Gosse and Phillips, 2001 for a discussion of this value). Given a typical density for granitic rocks (2.7 g cm$^{-3}$), the spallogenic production rate drops by a factor of two with every ~40 cm increment of depth and becomes negligible 2–3 m below the surface.

The third important point is that many geological processes act to bring subsurface rocks – which have not been exposed to the cosmic-ray flux and so do not contain significant cosmogenic-nuclide concentrations – to the surface where nuclide production can occur. The cosmogenic-nuclide concentration in a rock sample is subsequently proportional to the length of time that the sample has been exposed at the Earth's surface. This provides the foundation of the method of cosmogenic-nuclide exposure dating. Any event that brought fresh rock to the surface can be dated by measuring the cosmogenic-nuclide concentration in the surface created by that event. Taking the example of $^{10}$Be, which is produced by spallation of O and Si in quartz, the $^{10}$Be concentration in quartz that had a negligible $^{10}$Be concentration before it was exposed, and has been subsequently exposed at the surface without erosion, is

$$N_{10} = \frac{P_{10}}{\lambda_{10}}\left[1 - e^{-\lambda_{10}t}\right] \quad (2)$$

where $N_{10}$ is the $^{10}$Be concentration in quartz (atoms g$^{-1}$), $P_{10}$ is the $^{10}$Be production rate (atoms g$^{-1}$ yr$^{-1}$) in quartz at the sample site, $\lambda_{10}$ is the $^{10}$Be decay constant ($4.99 \times 10^{-7}$ yr$^{-1}$), and $t$ is the exposure time (yr). Given a measurement of the $^{10}$Be concentration and knowledge of the production rate at the site, this can be solved to yield the exposure time.

The initial challenges in applying this relationship to carry out exposure dating were i) to accurately measure the concentration of cosmogenic nuclides, most of which occur at extremely low concentrations on the order of thousands to hundreds of thousands of atoms g$^{-1}$ of the target mineral, and ii) to estimate the production rates of these nuclides. These two tasks have been accomplished for a number of stable nuclides and radionuclides, mainly $^{3}$He, $^{10}$Be, $^{14}$C, $^{21}$Ne, $^{26}$Al, and $^{36}$Cl. All these have been used for glacial chronology, but the low detection limit and straightforward production systematics of $^{10}$Be mean that this nuclide has the best determined production rate, is most precisely measured at low concentrations, and is most widely used for glacial chronology; most of the examples to be discussed here involve $^{10}$Be.

### 2.2. Why cosmogenic-nuclide dating is useful for glacier chronology

Exposure dating is useful for dating glacier advances and retreats because glaciers create fresh rock surfaces. First, so-called 'temperate' glaciers – those glaciers whose beds are at the pressure-melting point of ice, so that free water is present – are very effective agents of erosion. Rapid erosion of rock takes place at glacier beds. Because the bed of a glacier is also shielded from the cosmic-ray flux by the overlying ice, subglacial erosion acts to create fresh rock surfaces whose cosmogenic-nuclide inventory is negligible. This is also true of the products of subglacial erosion. Clasts detached from an actively eroding glacier bed and subsequently transported by ice can also be expected to have a negligible cosmogenic-nuclide concentration. When these are transported to the ice margin and deposited as a moraine, or when either subglacially derived clasts or deeply subglacially eroded surfaces are uncovered by ice retreat, they become exposed to the cosmic-ray flux and begin to accumulate cosmogenic nuclides. This means that cosmogenic-nuclide exposure dating can be used to date moraine emplacement as well as ice retreat.

## 3. Rapid expansion of cosmogenic-nuclide applications to glacial chronology worldwide

The key ingredients for wide application of exposure dating were the development of measurement techniques capable of measuring low enough concentrations of cosmic-ray-produced nuclides, and the ability to estimate nuclide production rates at any location worldwide. Improvements in accelerator mass spectrometry (AMS) and noble gas mass spectrometry in the late 1980s provided the technology needed for measurement of $^{10}$Be, $^{26}$Al, $^{3}$He, and $^{36}$Cl at the levels found in Earth surface materials (see review in Elmore and Phillips, 1987). This in turn permitted estimates of nuclide production rates by measurement of their concentrations in surfaces of known age (Phillips et al., 1986; Nishiizumi et al., 1989; Kurz et al., 1990), and the geographic scaling scheme of Lal (1991) allowed scaling these production-rate estimates to any site. With these ingredients in place, Phillips et al. (1990) could carry out the first large-scale study of glacier chronology with cosmogenic-nuclide

exposure dating, using measurements of cosmogenic $^{36}$Cl to date boulders on the Bloody Canyon moraine sequence at the eastern front of the California Sierra Nevada.

Since that time AMS measurement of cosmogenic nuclides, primarily $^{10}$Be, $^{26}$Al, and $^{36}$Cl, has become routine and widely available to glacial geologists. The result of this availability is that cosmogenic-nuclide exposure dating has by now been used to date glacial deposits nearly everywhere on Earth (Fig. 1). I attribute this extremely rapid adoption of the method, and proliferation of exposure ages on glacial deposits, to the fact that cosmogenic-nuclide exposure-dating filled two pre-existing needs already recognized by glacial geologists.

First, well before the development of cosmogenic-nuclide exposure dating, glacial geologists had already exploited "exposure dating" in a general sense to date glacier retreat. The processes of revegetation and weathering after a fresh rock surface is exposed by ice retreat mean that many easily observed metrics such as the age of trees, the size of lichens, or the thickness of weathering rinds are related to the "exposure age" of the surface. Observations of this sort had already been applied extensively to date glacier advances and retreats (e.g., Blackwelder, 1931; Beschel, 1950; Lawrence, 1950; Brigham-Grette, 1996, and references therein). All of these methods, however, suffer from at least one of two failings. One is that many of them reach saturation quickly. For example, lichens can become large enough to interfere with each other, or the first generation of trees can die off, only a few decades after exposure. The other is that the rates at which these indicators of exposure duration develop are site-specific. For example, the time required for trees to colonize fresh surfaces depends on hydrology and climate; the rate of lichen colonization and growth depends on the substrate and the microclimate in which the lichens are growing, so lichen growth rates calibrated at one location cannot be used at another; and chemical weathering processes depend on rock type, temperature, and water availability. Cosmogenic-nuclide exposure dating has a much longer potential time range than most of these methods and, more importantly, overcomes the limitation of site-specificity because nuclide production rates can be related from site to site based on physical principles.

Second, prior to the advent of exposure dating, most glacial chronologies relied on radiocarbon dating. Because radiocarbon measurements can be made very precisely, and because of decades of exhaustive research into the calibration of radiocarbon dates to the calendar year time scale, radiocarbon-based glacier chronologies are potentially more accurate than even the current state-of-the-art exposure-dating studies. However, they have two disadvantages. The main one is that glacier advances do not themselves create organic material, so radiocarbon dates by nature provide the age of either organic material that lived prior to a glacier advance, or organic material that lived after a glacier retreat. They can provide bracketing ages only. Cosmogenic-nuclide exposure dating overcomes this limitation because the event we wish to date is the same event that starts nuclide accumulation in a fresh surface, so (in the absence of geological complications discussed later) exposure ages provide

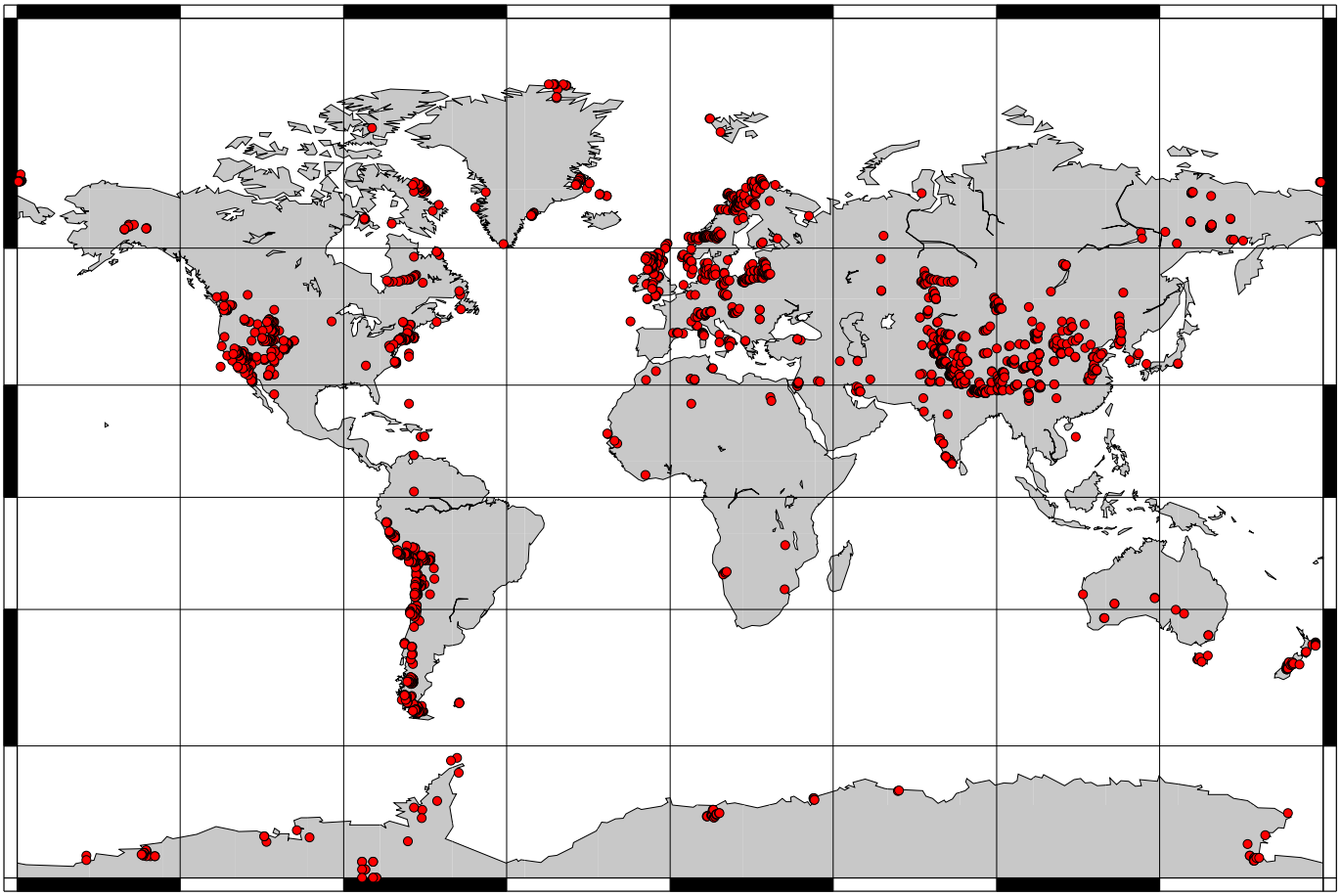

**Fig. 1.** Locations of exposure-age measurements whose age was calculated using the CRONUS-Earth online exposure-age calculator (Balco et al., 2008) between 2007 and 2010. The only information permanently recorded by the online system is the sample location, so it is not possible to determine how many of these sample locations correspond to published studies of glacier chronology. In addition, it is likely that some of these sample locations reflect incorrect data entry. However, it is clear that cosmogenic-nuclide exposure-dating studies have been carried out in most glaciated regions of the world.

direct rather than bracketing ages. The second is that glaciers by nature occur in polar or alpine environments where vegetation is scarce, so only a minority of glaciers leave deposits that can be radiocarbon dated at all. Cosmogenic-nuclide exposure dating overcomes this limitation because, with only a few exceptions, all glaciers generate fresh rock by erosional processes and transport it to their margin.

To summarize, cosmogenic-nuclide exposure dating met several needs already recognized by glacial geologists, so little new geological or geomorphic understanding was needed to encourage its adoption. In addition, the relative ease and speed of collection of surface rock samples from obvious landforms, compared with the careful search and coring, drilling, or excavation usually required to obtain close bracketing radiocarbon ages, provided a further incentive to the proliferation of exposure-dating studies. At present it is unusual to find a study of glacier chronology that does not rely primarily on exposure dating.

### 3.1. Recognition of inheritance; convergence on moraine boulder dating

At first, both exposure-dating studies and simultaneous efforts to calibrate nuclide production rates (by measuring nuclide concentrations at sites exposed by already-radiocarbon-dated glacier retreats) targeted both glacially transported boulders, mostly on moraines, and glacially polished or striated surfaces exposed by ice retreat (e.g., Nishiizumi et al., 1989; Clark et al., 1995). Some (but not all) of these studies found that nuclide concentrations in glacially polished surfaces were often much greater than in nearby glacially transported boulders, and in fact could be many times greater than permitted by the time available since deglaciation (Briner, 1998; Bierman et al., 1999, see Fig. 2). Although the theory of subglacial erosion (Hallet, 1979, 1986) already predicted that subglacial erosion rates due to the process of abrasion were likely to be rather low, these results were a striking demonstration of i) the fact that subglacial erosion was often inadequate to remove cosmogenic-nuclide inventories produced during previous ice-free periods, and ii) the difference between rates of subglacial erosion by abrasion and by plucking (Briner, 1998). Abrasion is certainly effective sometimes, and many examples also exist in which nuclide inventories in striated surfaces are commensurate with the deglaciation age of the surface (e.g., Nishiizumi et al., 1989; Clark et al., 1995; Kelly et al., 2006). However, the key conclusion one can draw from these studies is that there is no obvious way to determine in advance of sampling whether a striated bedrock surface has been fully reset by subglacial erosion or not. This has discouraged most researchers from relying on exposure ages from polished bedrock sites, and the majority of current and recent exposure-dating studies has relied on either bedrock surfaces where subglacial erosion was by plucking rather than abrasion, or, more commonly, on glacially transported cobbles and boulders.

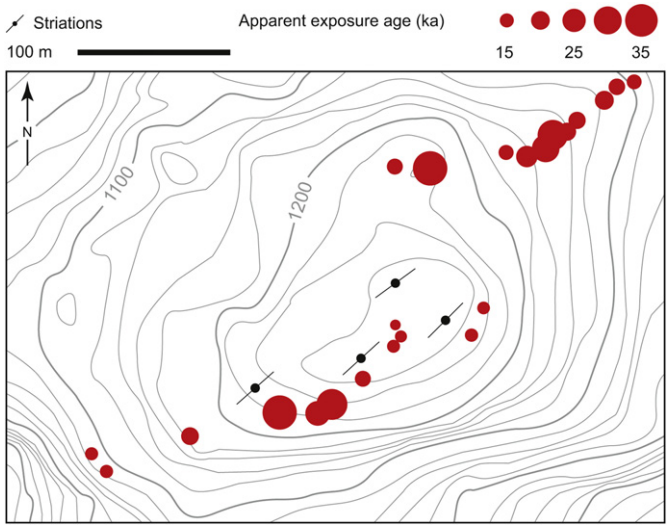


**Fig. 2.** $^{36}$Cl exposure ages from Mt. Erie, northwestern Washington, US (48°27′ N, 122°37′ W), described in Briner (1998), that show incomplete resetting of cosmogenic-nuclide inventories by subglacial erosion. This landform is a streamlined bedrock hill that was covered by the Puget Lobe of the Cordilleran Ice Sheet. Ice flowed from northeast to southwest. A radiocarbon chronology shows that it was exposed by ice retreat 15,000 years ago. However, the apparent exposure ages of many parts of the bedrock surface are well in excess of this age, because subglacial erosion of these areas was inadequate to remove the $^{36}$Cl inventory produced during previous ice-free periods. Elevation contours are in feet.

### 3.2. Special mention of Antarctica

The obstacles to radiocarbon dating of glacial deposits, specifically the lack of organic material in alpine and polar regions, are most severe in Antarctica where terrestrial flora and fauna are essentially absent. At the same time, because the Antarctic ice sheet is the largest potential contributor to future sea-level change, understanding Antarctic ice sheet history is extremely important. This combination of importance and difficulty inspired a number of radiocarbon-dating studies in Antarctica that were notable for their exhaustive and heroic efforts to search out rare and unlikely material – finely disseminated algae in glacial deposits (Bockheim et al., 1989; Hall and Denton, 2000), elephant seal hair (Hall et al., 2006), and penguin eggshell (Emslie et al., 2007) among them – that could be dated. Even with these efforts, however, radiocarbon-dateable material has only been found at a tiny minority of the many ice-free areas in Antarctica where geologic evidence of past ice sheet changes is preserved.

On the other hand, the Antarctic environment is nearly perfectly suited to cosmogenic-nuclide exposure dating of glacial deposits. Because there are very few ice-free areas in Antarctica, nearly all englacial debris is subglacially derived and thus is unlikely to have experienced prior exposure to cosmic rays. Once glacially transported clasts are deposited at the ice margin, the arid and windy climate means that they are not likely to be covered by snow or disturbed by weathering or periglacial processes. Thus, nearly any surficial glacial deposit in Antarctica is suitable for cosmogenic-nuclide exposure dating, which permits a vastly more comprehensive reconstruction of ice sheet change than could be possible only from radiocarbon dates.

At first, exposure-dating studies in Antarctica were directed at solving specific geochronological problems that had emerged from existing stratigraphic and geomorphic research. As the method was being developed in the early 1990s, a main focus in Antarctic glacial geology concerned the Miocene through Pleistocene history of the East Antarctic Ice Sheet, as recorded by glacial deposits in the Transantarctic Mountains (e.g., Denton et al., 1993; Stroeven and Prentice, 1997). Correlation with dated volcanic ashes showed that some of these deposits had been exposed near the surface for millions of years (see Marchant et al., 1996), so they were expected to have extremely high cosmogenic-nuclide concentrations that could be precisely measured with the capabilities that were available at the time. In fact this was the case, and early applications of cosmogenic-nuclide dating to Transantarctic Mountains glacial deposits were important in i) developing the technique and showing that exposure-dating results were consistent with other lines of evidence for long surface exposures; ii) quantitatively verifying the extremely low erosion rates responsible for the long-term survival of surficial deposits in this environment, and iii) helping to resolve conflicting evidence regarding a suggested Pliocene collapse of the East

Antarctic Ice Sheet that motivated much of this research in the first place (Bruno et al., 1997; Schäfer et al., 1999).

As the precision and detection limit of cosmogenic-nuclide measurements improved, it became clear that the method could be used not only on the very old glacial deposits relevant to Plio-Pleistocene ice sheet history, but also on the youngest glacial deposits in Antarctica that record the thickness of the ice sheet at the Last Glacial Maximum (LGM), and its subsequent shrinkage to its present thickness. This information is necessary for understanding past and present sea-level change, but cannot be obtained from existing radiocarbon dates. Ackert et al. (1999) first implemented this idea, using cosmogenic-nuclide exposure dating of glacial erratics preserved on nunataks at the center of the West Antarctic Ice Sheet to show that this ice sheet was thinner, and reached its maximum extent later, than accounted for in existing sea-level reconstructions. Subsequently Stone et al. (2003) used essentially the same approach, but collected a much larger data set, to reconstruct the LGM-to-Holocene thinning history of the Ford Ranges in West Antarctica from exposure ages of glacial erratics preserved on nunataks (Fig. 3). This work made it clear that it was potentially possible to reconstruct the LGM-to-Holocene elevation change history of the Antarctic ice sheets nearly anywhere that nunataks were present, and extensive subsequent research has aimed to apply this idea throughout the Antarctic continent (Johnson et al., 2008; Bentley et al., 2010; Todd et al., 2010). In my opinion, these studies represent the most significant contribution of cosmogenic-nuclide exposure dating of glacial deposits yet. Exposure-dating studies of glacial deposits elsewhere in the world have, with a few exceptions, refined a glacial history that was already approximately known from existing radiocarbon chronologies. However, exposure-dating studies in Antarctica have revealed an LGM-to-Holocene ice sheet change history that was essentially unknown, but is critically important to understand past sea-level change. Without these studies, it would not be possible to correctly evaluate the importance of Antarctic ice sheet change to LGM-to-Holocene meltwater input to the oceans (e.g., Ivins and James, 2005, and references therein).

## 4. Concomitant methodological developments

### 4.1. Improvements in mass spectrometry and sample preparation

Measurement of cosmic-ray-produced nuclides involves two main analytical techniques: accelerator mass spectrometry (AMS) for the radionuclides $^{10}$Be, $^{26}$Al, $^{36}$Cl, and others; and noble gas mass spectrometry (NGMS) for the stable nuclides $^{3}$He and $^{21}$Ne. These two measurement techniques face different technical challenges. For the stable noble gases, the major obstacle to accurate measurement of cosmic-ray-produced $^{3}$He or $^{21}$Ne is resolution of cosmogenic from trapped nuclide inventories (e.g., Niedermann, 2002, and references therein). Thus, the accuracy of the measurement relies more on accurate isotope ratio measurements at signals well above background than on the detection limit or the instrument blank. In effect the signal-to-noise ratio is determined by the characteristics of the sample, rather than of the instrument. For this reason, the recognition that it was possible to measure cosmogenic noble gases was not a consequence of a fundamentally new technology – NGMS systems were already a fairly mature technology at the time – but of ongoing research into isotope systematics of trapped gases in minerals. Since that time, there have been incremental improvements in the sensitivity of NGMS systems, but no major improvements that have fundamentally changed the type of samples that could be analysed, or the class of research questions that could be addressed.

Developments in measurement of the cosmogenic radionuclides by AMS have been more dramatic. In contrast to the cosmogenic noble gases, the radionuclides are generally less abundant, but have lower background concentrations in natural materials. Thus the growth in applications of the cosmogenic radionuclides has depended almost entirely on the initial development of AMS measurements, the gradual increase in measurement precision as AMS systems themselves have improved, and the lowering of blanks and detection limits as chemical preparation and extraction techniques have evolved. The precision of AMS measurements primarily depends on the efficiency of the AMS ion source in converting the element of interest – Be for example – into an ion beam that can be transmitted through the mass spectrometer and detected. In the example of $^{10}$Be, ion source efficiency has improved for two reasons: first through steady but gradual improvements in the understanding of source design and tuning, but also through a single serendipitous discovery that improved ion beam currents by several times. The latter relates to the method of preparing Be targets for AMS isotope ratio measurement. Be is extracted from a sample as BeO, which must be combined with a conductive metal binder before being sintered into the cathode of an AMS ion source. Initially, silver was used as the binder. In approximately 2000, researchers at an Australian AMS facility (Fink et al., 2000) discovered that using niobium metal powder as the binder increased the efficiency of their ion source by a factor of 3–7 (see

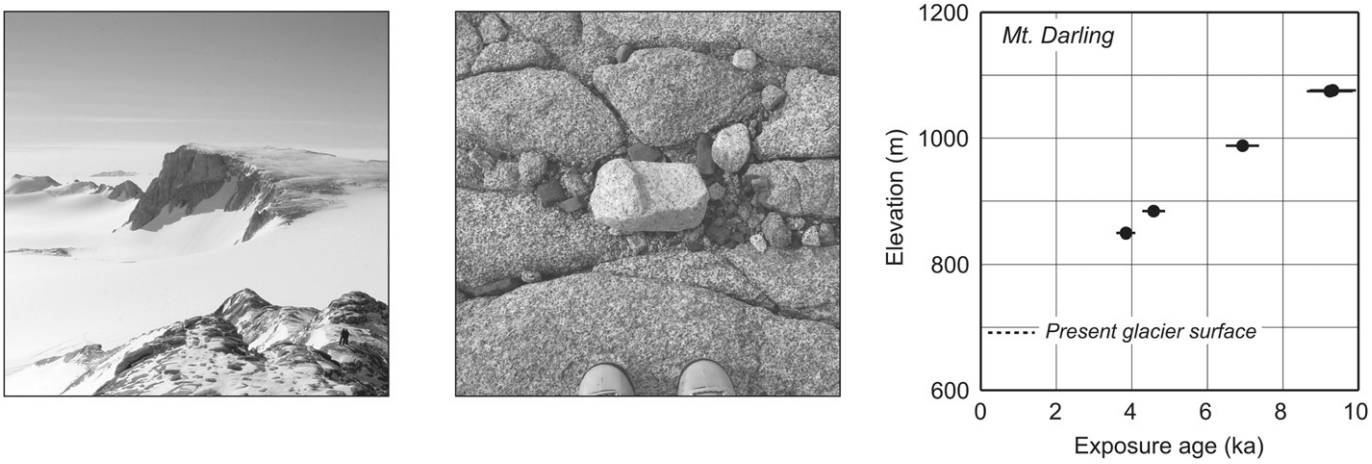


**Fig. 3.** Exposure ages from erratic cobbles stranded on nunataks in West Antarctica that record steady Holocene ice surface lowering, from Stone et al. (2003). Image at left shows Mt. Darling, a nunatak in the Ford Ranges of Marie Byrd Land (77°15′ S, 143°20′ W). Center image shows a typical erratic cobble from the Ford Ranges. Right panel shows exposure age – elevation relationship for erratics on Mt Darling. Exposure ages increase with elevation, recording steady Holocene ice surface lowering and emergence of the nunatak.

also Hunt et al., 2008, and references therein). The majority of AMS labs has now adopted this method, which has improved the attainable measurement precision for Be isotope ratio measurements (to better than 1% in some cases) and decreased the time required for analysis, thus enabling faster sample throughput.

Even before the development of the BeO–Nb cathode, however, the detection limit for $^{10}$Be, as well as the measurement precision for concentrations near the detection limit, was set not by the characteristics of the AMS system but by the chemical processing method used for extracting Be from quartz samples. $^{10}$Be is measured by an isotope dilution method in which a known quantity of $^{9}$Be carrier is added to the sample at the time of dissolution, the added $^{9}$Be equilibrates with the natural $^{10}$Be released by dissolution, and then all Be is extracted from the solution and its isotope ratio is measured. During the 1980s and 1990s, nearly all researchers used commercially available Be standard solutions as the $^{9}$Be carrier. However, nearly all commercially available Be contains a significant amount of $^{10}$Be, having a $^{10}$Be/$^{9}$Be ratio near $10^{-14}$. This ratio is two orders of magnitude above the detection limit for AMS systems and, given typical sample and carrier weights, yields a $^{10}$Be abundance in chemical process blanks that is a significant fraction of the natural $^{10}$Be abundance in typical Holocene and Lateglacial samples. Stone (1998) showed that one could make a $^{9}$Be carrier solution from deep-mined beryl that had a $^{10}$Be/$^{9}$Be ratio near $10^{-16}$, and such a carrier solution was used by Stone et al. (2003) and others including Schaefer et al. (2009) to make relatively precise $^{10}$Be measurements on samples exposed for only a few hundred years. To summarize, these two parallel improvements in AMS measurement and chemical preparation of $^{10}$Be have significantly decreased the detection limit and improved precision across the range of natural $^{10}$Be concentrations (Fig. 4). This in turn has allowed the method to be used on younger and younger samples, to the extent that exposure-age chronologies for glacier change can now overlap with historical observations (e.g., Schaefer et al., 2009).

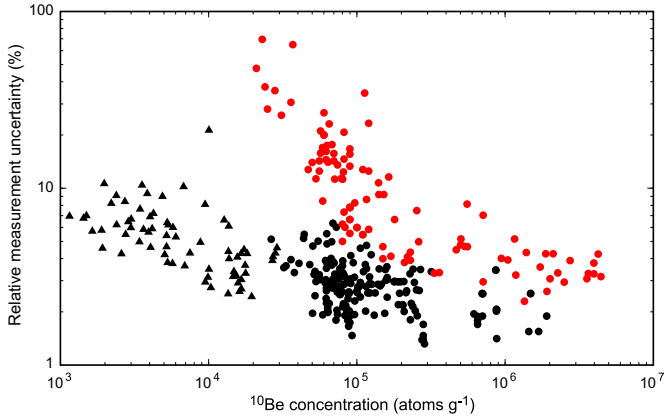


**Fig. 4.** Improved precision in $^{10}$Be measurements due to advances in sample preparation and AMS isotope ratio measurement. Red circles show $^{10}$Be measurements from the 1990s made by Bierman et al. (1995), Bierman and Turner (1995), Marsella (1998), and Marsella et al. (2000). These measurements represent the approximate state-of-the-art at the time, and share two features: they employed a commercially available $^{9}$Be carrier with $^{10}$Be/$^{9}$Be $\simeq 1 \times 10^{-14}$, and the AMS isotope ratio measurements were made at the Center for Accelerator Mass Spectrometry, Lawrence Livermore National Laboratory (LLNL-CAMS) on AMS cathodes prepared with a BeO–Ag mixture. It is clear that the precision of these measurements is limited by the $^{10}$Be blank contributed by the $^{9}$Be carrier. The black circles and black triangles show more recent $^{10}$Be measurements compiled from (i) samples analysed by the author in the University of Washington Cosmogenic Nuclide Lab (circles), and (ii) samples analysed by Schaefer et al. (2009) (triangles). These employed a $^{9}$Be carrier made from deep-mined beryl according to the recipe of Stone (1998), with $^{10}$Be/$^{9}$Be $\simeq 2–6 \times 10^{-16}$. AMS measurements were also made at LLNL-CAMS, but the cathodes were prepared with a BeO–Nb mixture. Increased beam currents resulting from the Nb cathodes improve precision at all levels, and the low-blank carrier permits precise measurements at lower concentrations. No effort is made in this plot to correct for sample size; this is presumably responsible for most of the scatter in both data sets.

### 4.2. Resolution of standardization issues

A related methodological development concerned the AMS isotope ratio standards used for $^{10}$Be measurements. Like most mass-spectrometric measurements, AMS isotope ratio measurements do not directly measure the absolute isotope ratio of a sample, but compare the isotope ratio of a sample to that of a standard whose absolute isotope ratio is already known. Typically one creates such a standard by obtaining a stock of Be whose $^{10}$Be/$^{9}$Be ratio has been highly enriched by irradiation, determining the total amount of Be by gravimetric methods, and then determining the amount of $^{10}$Be by decay counting. This requires knowledge of the $^{10}$Be half-life. Until recently, independent measurements of the $^{10}$Be half-life, although individually precise, differed by ~10%. The fact that the $^{10}$Be half-life was not well known did not by itself present a significant obstacle to exposure dating of glacial deposits, because most glacial deposits that have been exposure-dated have exposure ages that are short relative to the $^{10}$Be half-life. The issue that is important for exposure dating is that the absolute isotope ratio of a Be AMS standard that was prepared as described above does depend on the value of the $^{10}$Be half-life that was used to compute the ratio. Thus, a $^{10}$Be concentration in an unknown sample measured against a standard defined with reference to one value of the half-life would not be directly comparable with a concentration measured against a standard defined by reference to a different half-life. This did not present a significant difficulty in the earliest days of exposure dating of glacial deposits, mainly because early applications of the method were focused on questions that could be answered with measurements at ~10% precision. However, five developments led to this issue becoming a serious difficulty in the interpretation and synthesis of exposure-dating results: i) the commissioning of more AMS facilities and corresponding increase in the number of isotope ratio standards in use, ii) the improving precision of AMS measurements, iii) the widespread use of AMS measurements by geologists who were not familiar with the preparation of isotope ratio standards, iv) poor data reporting in the exposure-dating literature, and v) the widespread adoption of $^{10}$Be as the nuclide of choice for most exposure-dating studies. The effect of these factors was a proliferation of both $^{10}$Be production-rate calibration measurements and $^{10}$Be exposure-dating results that were normalized to different AMS standards and in many cases poorly documented. This in turn led to a situation where one could unknowingly compute exposure ages from $^{10}$Be measurements made against one standard using production rates originally measured against another standard, leading to incorrect results. It is certain that many such examples occur in the exposure-dating literature published between approximately 1998 and 2007, and in some cases they cannot be identified and corrected using published data.

As the number of $^{10}$Be measurements on glacial deposits increased, interest in comparing these data sets and in synthesizing these results into broader paleoclimate syntheses also increased. This could not be done without a means of interrelating inconsistent AMS standardizations, which in turn required three tasks: first, the two linked tasks of determining the correct half-life for $^{10}$Be and of comprehensively intercalibrating all available AMS standards; second, increasing the attention paid to data reporting in the exposure-dating literature. Nishiizumi et al. (2007) addressed the first two tasks. They decoupled the issue of what the $^{10}$Be half-life actually was from the issue of what the absolute isotope ratios of AMS standards were by using the Lawrence Livermore National Laboratory AMS to implant a precisely counted number of $^{10}$Be

atoms in a silicon wafer, which could then be dissolved and diluted with a known quantity of $^{9}$Be. The result was a stock of Be whose isotope ratio was known independently of any assumptions about the $^{10}$Be half-life. They could then use this material as a measurement standard to determine the absolute isotope ratios of other AMS standards. This work, along with several other intercomparison studies (e.g., Kubik and Christl, 2010) finally permitted a consistent intercomparison of $^{10}$Be measurements made against different AMS standards. The final task, that of improving the state of data reporting in the exposure-dating literature, has recently been the subject of numerous publications that seek to call attention to the problem of incomplete data reporting and instruct users in how to fix the problem (Balco et al., 2008; Dunai, 2010; Dunai and Stuart, 2010; Frankel et al., 2010). Thus, even though there still exist many published exposure-dating results that did not record the standard used for their AMS measurements (so they remain uninterpretable to present and future researchers), it is now possible to compare the majority of exposure-dating measurements on glacial deposits in a consistent fashion. This, with the development of standardized calculation methods discussed below, has finally permitted this large data set to be used in paleoclimate syntheses.

### 4.3. Production-rate measurements and scaling

The two requirements for an accurate cosmogenic-nuclide exposure age are an accurate measurement of nuclide concentration, and an accurate estimate of the nuclide production rate. The steady improvements in AMS measurement technology just discussed have better and better addressed the first of these requirements. The second, accurate production-rate estimates, has also been the subject of a large amount of development research in the last two decades. In principle it would be possible to compute cosmogenic-nuclide production rates everywhere on Earth from a first-principles physical simulation of the cosmic-ray flux to the surface (e.g., Masarik and Reedy, 1995). However, this is not practically feasible at present, not only because of the complexity of this calculation, but because very few of the cross-sections for the spallation reactions that produce the nuclides of interest have been accurately measured. Estimating cosmogenic-nuclide production rates at the site of an exposure-dating sample thus involves a combination of first-principles physics, empirical observations of the present-day cosmic-ray flux, and empirical measurements of long-term production rates from nuclide concentrations in surfaces with independently dated exposure ages. These elements can be summarized into two requirements: a scaling scheme, which describes the variation in nuclide production rates with geographic location, elevation, and time; and a calibration data set, which consists of nuclide concentrations measured in one or more surfaces whose exposure age is known independently. The first widely used scaling scheme was developed by Lal (most comprehensively described in Lal, 1991), and consists of a set of analytical functions fit to a variety of observations of the cosmic-ray flux. The arguments to the functions are latitude (as a proxy for geomagnetic field properties) and altitude (as a proxy for atmospheric depth). At approximately the same time, Kurz et al. (1990) provided a calibration data set (from dated lava flows in Hawaii) for $^{3}$He production in olivine, Nishiizumi et al., 1989 provided one for $^{10}$Be and $^{26}$Al in quartz (from glacially eroded surfaces in the California Sierra Nevada), and Phillips et al. (1986) and Zreda et al. (1991) for $^{36}$Cl (mainly from lava flows in the western U.S.). These studies provided the minimum necessary ingredients to apply cosmogenic-nuclide exposure dating to glacial deposits worldwide, and the majority of exposure-dating studies of glacial deposits between approximately 1990–2001 used one of these calibration data sets with the Lal scaling scheme.

At the same time, many other researchers developed new production-rate calibration data sets from a wide range of globally distributed sites. This was the case for all commonly used cosmogenic nuclides, but I will focus on $^{10}$Be as an example. New $^{10}$Be production-rate calibration data sets were generated from an Austrian landslide by Kubik et al. (1998), from glacial moraines in Wyoming by Gosse et al. (1995), from glacial deposits in Scotland by Stone et al. (1998), from the terminal moraines of the Laurentide Ice Sheet in New Jersey by Larsen (1996), from the shorelines of glacial Lake Bonneville by Gosse and Klein (1996), and from artificial target experiments by Nishiizumi et al. (1996). In principle, if the key geological assumptions that go into a production-rate calibration site (mainly that the surface has been undisturbed during the period of exposure) are valid, if the independent dating is correct, and if the scaling scheme correctly describes the geographic variability of production rates, then one should be able to use the scaling scheme to scale all calibration data to a common location and obtain the same result. However, the Lal scaling scheme could not achieve this for these calibration data sets. Stone (2000) then pointed out that two modifications to the Lal scaling scheme – casting the Lal polynomials as functions of mean atmospheric pressure rather than elevation, and adjusting the proportion of production due to muon interactions – could correct this problem and bring all calibration data sets into decent agreement (Fig. 5). Henceforth the most commonly used means of estimating the $^{10}$Be production rate was to use the Lal/Stone scaling scheme with this combined global calibration data set.

Beginning with Dunai (2000), however, several researchers noted that the elevation dependence of production rates represented in the Lal and subsequent Lal/Stone scaling schemes was at odds with that inferred from more recent measurements of the modern cosmic-ray flux using neutron monitors. This led to the development of several new scaling schemes (Dunai, 2000, 2001; Desilets and Zreda, 2001, 2003; Lifton et al., 2005, 2008; Desilets et al., 2006) that differed from the Lal/Stone scheme. These scaling schemes also emphasized the fact that the Earth's magnetic field changes over time, which causes corresponding changes in cosmogenic-nuclide production rates. Nishiizumi et al. (1989) had already adapted the Lal scaling scheme to deal with this observation by incorporating a simple relation between magnetic field strength and geomagnetic latitude, but these new schemes represented production-rate scaling as functions of both geomagnetic cutoff rigidity (a quantity related to magnetic field strength) and mean atmospheric pressure, and incorporated fairly complex time-dependent models of the Earth's magnetic field to predict production-rate variation as a function of location, elevation, and also time.

This period of development of new scaling schemes had two effects. First, by 2005, glacial geologists interested in computing exposure ages had to choose among four widely used scaling schemes and at least seven different production-rate calibration studies to estimate $^{10}$Be production rates at their sites. In addition, many of these calibration studies represented production rates not as local production rates at the calibration site, but as production rates normalized to sea level and high latitude. This implies the use of a particular scaling scheme to carry out the normalization, and complicates use of the calibration data with a different scheme. All these developments made it easy for nonspecialists to inadvertently choose a reference production rate and a scaling scheme that were not internally consistent and would lead to wrong exposure ages.

Second, applying these new scaling schemes to existing and new production-rate calibration measurements made it clear that the newer scaling schemes, although they included more realistic representations of magnetic field structure and changes and

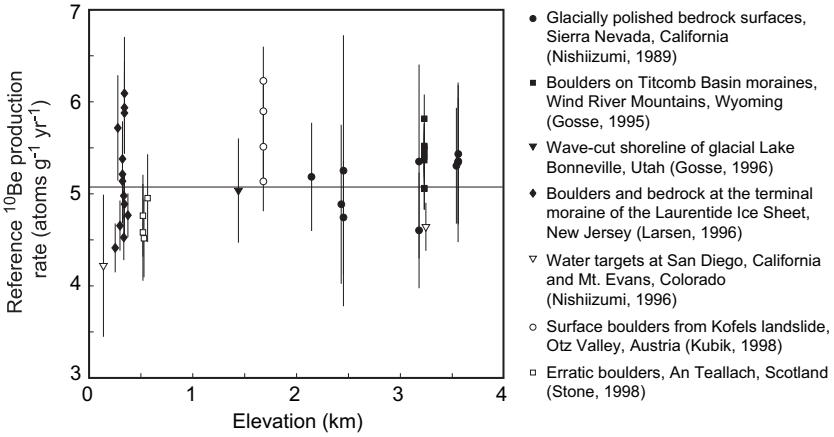


**Fig. 5.** State of $^{10}$Be production-rate calibrations in 2000. This plot shows total $^{10}$Be production rates inferred from all samples analysed in seven production-rate calibration studies that were available at the time, scaled to a reference production rate at sea level and high latitude according to the scaling scheme of Stone (2000). Despite considerable scatter within many of the data sets, all the scaled values showed reasonable agreement around a mean of 5.1 atoms g$^{-1}$ yr$^{-1}$. Note that nearly all production-rate measurements are from temperate latitudes between ~40 and 50°N, so this is not a very stringent test of the geomagnetic aspects of the scaling scheme.

appeared to give an improved fit to observations of the present-day cosmic-ray neutron flux, did not do a better job of reconciling production-rate calibration data than the original Lal scaling scheme (Fig. 6; also see discussion in Balco et al., 2008). For the majority of exposure-dating studies, different scaling schemes, even if used with a single calibration data set, will predict significantly different exposure ages for the same samples. The observation that none of these scaling schemes was clearly preferable to the others significantly added to the difficulty of choosing a scaling scheme and calibration data set, and generally highlighted the importance of systematic scaling uncertainties in the interpretation of exposure-age data.

### 4.4. Standard and internally consistent calculation methods

To summarize, this period of scaling scheme development and expansion of the production-rate calibration data set certainly increased physical and empirical knowledge of cosmogenic-nuclide production rates and their variations on geologic time scales, but made it somewhat more difficult for nonspecialist glacial geologists to compute exposure ages, and nearly impossible for paleoclimatologists to synthesize multiple exposure-dating studies in an internally consistent fashion. One needed to choose among a variety of scaling schemes and production-rate calibration data sets with little clear guidance as to which were the most accurate, and, in addition, the computations required to use some of these scaling schemes were now quite complex. The obvious potential remedy for this situation was to assemble some sort of straightforward and easy-to-use software tool that would allow all users to do two things: compute their own exposure ages according to generally accepted calculation methods; and recompute published exposure ages that had used different scaling schemes or production rates, so that different studies could be compared on a common basis.

As early as 1996, Clapp and Bierman (1996) recognized the value of producing a standard software tool to carry out the scaling calculations used in exposure dating, and distributed a program called “Cosmo-calibrate” that computed exposure ages using

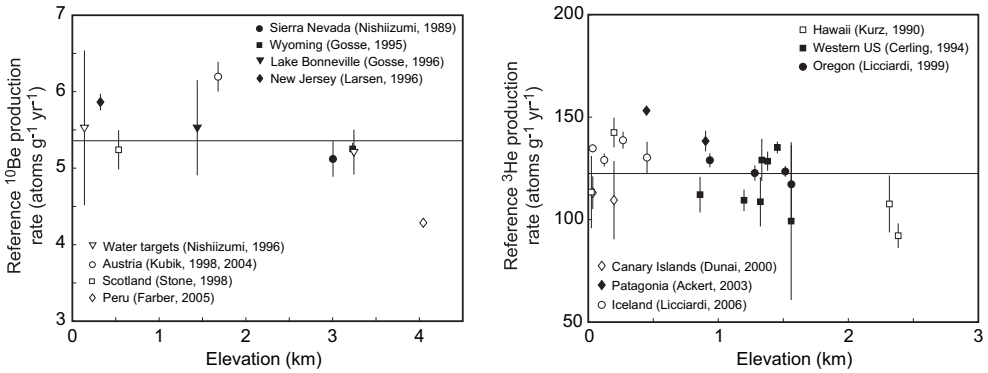


**Fig. 6.** State of $^{10}$Be and $^{3}$He production-rate calibration data sets in 2008. The left-hand plot, showing $^{10}$Be production-rate calibration data, is similar to Fig. 5 except that i) averages of all measurements from each calibration site are shown instead of all measurements, ii) it includes an additional production-rate calibration site (that of Farber et al., 2005) from a high-elevation site in Peru, and iii) a more recently developed scaling scheme is used to normalize the data to a sea level/high latitude reference value (that of Lifton et al., (2005), which is based on neutron monitor measurements and includes time-dependent corrections for magnetic field changes and solar variability). The right-hand plot shows $^{3}$He production-rate calibration data sets compiled in the same way and with the same scaling scheme. The Peru $^{10}$Be measurements, as well as $^{3}$He measurements from Hawaii, indicated that at least some scaling schemes – including ones that should in principle be more accurate because they include a more realistic treatment of magnetic field variations – could not reconcile the existing mid-latitude production-rate calibration data with those at high elevation and low latitude. This highlighted the potential for systematic errors in scaling schemes that could be masked by the relatively poor (~8–10%) measurement precision of many of the calibration data. $^{3}$He measurements are from Kurz et al. (1990), Cerling and Craig (1994), Licciardi et al. (1999), Dunai and Wijbrans (2000), Ackert et al. (2003), and Licciardi et al. (2006). The details of data selection, averaging, and scaling scheme implementation appear in Balco et al. (2008).

a paleomagnetically-corrected version of the Lal scaling scheme. At the same time Phillips and Plummer (1996) produced and distributed an Excel spreadsheet for computing $^{36}$Cl production rates and exposure ages. These both predated the above-discussed proliferation of scaling schemes and production-rate calibration data sets. Subsequently Lifton et al., (2005) provided a spreadsheet that implemented their scaling scheme; Schimmelpfennig et al. (2009) provided an updated spreadsheet for $^{36}$Cl exposure-age calculations; and Vermeesch (2007) distributed a comprehensive spreadsheet program that carried out a wide variety of scaling operations, exposure age and erosion rate calculations, and comparisons between multiple nuclides. Finally, the "ACE" software (*ace.hwr.arizona.edu)* is an extremely general collection of software tools that enables nearly any calculation related to cosmogenic-nuclide production, but is designed primarily as a development system for specialists. These programs solved the problem of providing relatively complex scaling computations to nonspecialist users, but allowed users to enter the reference cosmogenic-nuclide production rates of their choice. Thus, they did not solve the problem of choosing from the large menu of existing production-rate calibration data sets, and they permitted users to inadvertently choose production rates and scaling schemes that were not mutually consistent and would thus yield incorrect results. Balco et al. (2008) provided yet another set of software designed to calculate exposure ages and erosion rates from $^{10}$Be and $^{26}$Al measurements, which differed from these other programs in that i) it was mainly intended to be used as an online service accessible with any Web browser, and ii) it used a slightly different overall approach designed to address these remaining problems. These authors compiled all existing $^{10}$Be and $^{26}$Al production-rate calibration studies into a single data set, and used this data set to generate and apply summary reference production rates compatible with each of several published scaling methods. In contrast to other available software, this system performed many fewer functions and did not permit experimenting with different production rates and other input parameters, but on the other hand ensured that production rates and scaling schemes used to compute exposure ages would always be internally consistent. Because of the emphases on internal consistency, online access, simplicity of data entry, and avoiding the need for the user to make technical decisions about parameter selection, this software was widely adopted by nonspecialist users, in particular those who wished to synthesize or compare many previously published exposure-dating data sets on a common basis. This software has been described as the "Wal-Mart" of exposure-age calculation software because its emphasis on ease of use at the expense of user choice is analogous to the manner in which the giant U.S. retailer has stamped out retail diversity by offering lower prices. However, its widespread use has facilitated the first syntheses of large sets of exposure-dated glacier chronologies for use in broader paleoclimate studies, for example those of Owen et al. (2008), Clark et al. (2009), and Rodbell et al. (2009). This in turn is necessary for realizing the potential contributions of exposure-dated glacial chronologies to broader research questions.

## 5. Interaction between methodological improvements and applications

In the rest of this paper I focus on two issues. First, the increasing availability and improving precision of AMS measurements encouraged researchers to ask more detailed questions, that required more precise answers, about the timing of glacier advances worldwide and their relationship to other climate events. Second, these factors also revealed and highlighted two difficulties that made it harder to answer these questions: scatter in exposure ages from glacial landforms due to geologic processes (henceforth, "geologic scatter"), and inaccuracies in production-rate scaling schemes that make it difficult to correlate exposure-dated glacier chronologies with each other and with independently dated climate records.

The earliest applications of exposure dating to glacial chronologies focused on dating glacial deposits whose age was more or less entirely unconstrained, so even relatively imprecise ages represented a significant increase in knowledge. The first such study, that of Phillips et al. (1990), aimed to date a series of moraines in the California Sierra Nevada whose ages were for the most part unknown. The age of the youngest ("Tioga") moraine could be bracketed to 25–11 ka by radiocarbon dates, but age assignments for older moraines were largely speculative and based primarily on soil development, the degree of boulder weathering, and suggested correlations with the marine oxygen isotope record. Thus, any direct absolute age determination for these moraines, even if imprecise, represented important progress. Other studies in the 1990s that shared this approach include, for example, exposure dating of moraine sequences in the Antarctic Dry Valleys (Brown et al., 1991; Brook and Kurz, 1993), studies of the Sirius Formation in the Transantarctic Mountains that were aimed at determining whether it could or could not be late Pliocene in age (Bruno et al., 1997; Schäfer et al., 1999), and a study by Zreda et al. (1999) that sought to determine whether or not the Nares Strait between Greenland and Ellesmere Island was ice-covered during the Last Glacial Maximum.

Many more recent studies also fall into this category, where so little prior chronological information existed that the results of the study provided important new information regardless of any analytical, geologic, production rate, or scaling scheme uncertainties. For example, the question of whether or not weathering boundaries in recently deglaciated polar regions represented LGM ice limits was resolved by the observation that erratics above the weathering boundaries had LGM exposure ages (Briner et al., 2003; Sugden et al., 2005). Uncertainties in exposure dating did not affect the conclusion that the erratics in question were emplaced at the LGM and not some previous glaciation, or, therefore, the conclusion that the weathering boundaries were englacial thermal boundaries rather than the LGM ice limit. The age of the terminal moraines of the Scandinavian and Laurentide Ice Sheets in northern Europe and northeastern North America, respectively, was only constrained by bracketing radiocarbon ages to a period of several thousand years. The exposure-dating studies of Balco et al. (2002) and Rinterknecht et al. (2006) improved the precision of these estimates no matter what uncertainties are taken into account. Before the studies of Ackert et al. (1999) and Stone et al. (2003), the post-LGM thinning history of the West Antarctic Ice Sheet was essentially unconstrained, and the important conclusions of these studies that the WAIS reached its maximum thickness much later than the East Antarctic Ice Sheet, and continued to contribute water to the oceans throughout the Holocene, are unaffected by uncertainties in their exposure ages. Exposure dating of alpine glacier moraines in Tibet and the Himalayas (summarized in Owen et al., 2002a) showed that LGM-age moraines were fairly close to present-day ice margins throughout the Tibetan Plateau. Even large uncertainties in the precise ages of these moraines did not affect the conclusion that a proposed LGM ice sheet covering the Tibetan Plateau could not have existed. All these research questions were well-posed in that their answers were not significantly affected by the uncertainties in relating measured nuclide concentrations to exposure ages and, in my view, studies of this type represent the most significant and lasting contributions of cosmogenic-nuclide exposure dating to glacier chronology so far.

In 1995, Gosse et al. (1995) measured the exposure age of ten boulders from the inner Titcomb Lakes moraine in the Wind River range of Wyoming. These exposure ages agreed with each other to

the degree expected from analytical uncertainty, and, with the production-rate calibration data and scaling scheme available at the time, these authors concluded that this moraine had an age and uncertainty of 11,400 ± 500 years. They proposed that the moraine recorded a glacier advance that was simultaneous with the Younger Dryas cold period widely recognized in northern Europe, which showed that this event was global or at least hemispheric in scope. As the geographic extent of the Younger Dryas and other millennial-scale Lateglacial and Holocene climate changes was an important controversy in the paleoclimate literature at the time (and remains so today), this study was a significant development for exposure dating because it showed that moraines could be dated with a formal measurement uncertainty that was, in principle, small enough to permit correlating them with millennial-scale climate events. Numerous subsequent studies adopted this idea, proposing correlations between millennial-scale climate changes and exposure-dated moraines in, for example, Alaska (Briner et al., 2002), Patagonia (Douglass et al., 2006), the Alps (Kelly et al., 2004), California (Owen et al., 2003b), and Tibet (Tschudi et al., 2003).

In contrast to the examples discussed at the beginning of this section (in which the important research questions were posed so that methodological uncertainties did not affect the overall conclusions), systematic methodological uncertainties in computing exposure ages from measured nuclide concentrations have a significant impact on the conclusions of any study that seeks to correlate exposure-dated glacier chronologies with millennial-scale climate changes. First, these correlations are affected by geologic uncertainties, that is, failures of the basic geologic and geomorphic assumptions involved in relating exposure ages to the true age of glacier advances or retreats. As discussed in Section 6 below, many exposure-dating studies have observed that apparent exposure ages of samples on a single landform scatter more than expected from measurement uncertainty only. This nearly always appears to reflect postdepositional disturbance of the samples by geomorphic processes such as rock surface erosion, erosion of sediment cover, or soil creep. The magnitude of excess scatter in apparent exposure ages on Lateglacial moraines is commonly on the order of thousands of years, which is similar to the duration and/or spacing of important Lateglacial climate events. Second, most research into production-rate scaling between Lal (1991) and Balco et al. (2008) has concluded that the total systematic uncertainty in production-rate scaling schemes is approximately 10%. For Lateglacial moraines between ca 10,000 and 15,000 years old, a 10% uncertainty is 1000–1500 years, which is equal to or greater than the length of most Lateglacial climate oscillations. Thus, the conclusions of any study that aims to correlate exposure-dated moraines with independently dated Lateglacial and Holocene climate events can change completely if one uses a different production-rate scaling scheme or calibration data set to calculate exposure ages. In Section 7 below, I give examples of this sensitivity and discuss strategies to mitigate it. To summarize, realizing the goal of correlating exposure-dated glacier chronologies with independently dated records of millennial-scale climate changes requires understanding and mitigating both geologic scatter and scaling uncertainties.

## 6. Geologic scatter

### 6.1. Examples of geologic scatter

The basic assumptions required to apply cosmogenic-nuclide exposure dating to glacial landforms are i) that the rock surfaces to be dated lacked any inherited nuclide inventory when first exposed at the ice margin, and ii) that they have remained uncovered, uneroded, and in their original configuration until the time of sampling. Of course, this second assumption is unlikely to be strictly true – at the very least, nearly all rock surfaces in any alpine area are covered by snow for some fraction of the year – so in effect one is assuming that the effects of disturbance, cover, or erosion are either negligibly small, or can be accurately quantified and corrected for. Large moraine boulders are the most common target for exposure dating of glacial landforms: the fact that these are most likely derived from subglacial erosion suggests that assumption (i) is true, and the fact that they are often intact, unweathered, and still perched atop moraines suggests that (ii) is also true. This was the premise of the first exposure-dating study of alpine glacier moraines by Phillips et al. (1990).

As it turned out, however, equal in importance to the chronological results of this study was the observation that these assumptions were not, in fact, always true. Two observations showed this: first, the scatter of exposure ages from any one moraine increased with the stratigraphic age of the moraine; second, samples from the stratigraphically oldest moraine had a younger mean age than samples from a cross-cutting moraine (Fig. 7). In broad terms, these observations required some process that caused the apparent exposure ages of boulders from a moraine to be younger than the true emplacement age of the moraine. This could occur in three ways. First, boulders could have moved since deglaciation (henceforth, "disturbance"). If they were exposed for a time in one orientation and then overturned so that a previously shielded lower surface was now uppermost, then the apparent exposure age of the boulder top would underestimate the age of initial boulder emplacement. Second, boulder surfaces could have been partially shielded from the cosmic-ray flux by material that is no longer present ("cover"). For moraine boulders, this would most likely reflect downslope sediment transport on the moraine acting to expose boulders that were initially buried at the time of moraine emplacement, but could also reflect temporary cover by loess or other mobile sediment. Seasonal snow also covers boulder surfaces, but in principle this can be quantified and corrected for if one assumes that the present snow climatology reflects the long-term average. However, this assumption might not be true. Third, boulder surfaces could erode due to weathering, frost-shattering, or fire spalling ("surface erosion"). Surface erosion is essentially the same as cover in that the rock surface that is exposed at present was shielded in the past by the rock that has been eroded; thus, the apparent exposure age of the present surface underestimates the true age the boulder was emplaced. Surface erosion rates for crystalline rocks in most alpine environments are relatively slow – typically 0.5–2.5 mm $ka^{-1}$ – but because it is difficult to accurately estimate them, this issue contributes significant uncertainty to exposure ages for LGM and older boulders (Fig. 8).

Hallet and Putkonen (1994) sought to explain and quantify the observations of Phillips et al. (1990) using a numerical model of moraine degradation that incorporated two of these processes: the gradual uncovering of moraine boulders by diffusive creep of the matrix making up the moraine, and the steady erosion of boulder surfaces. These processes act both to destroy the boulders that were originally present at the time of moraine emplacement and to bring to the surface new boulders that were originally buried within the moraine. The model correctly predicts both phenomena observed in the Phillips study: the widening of apparent exposure-age distributions as new boulders are exposed and old ones weathered, and the eventual age inversion in the very oldest moraines where no original boulders survive.

These two studies provided a striking demonstration that, in addition to revealing new information about glacier chronology, cosmogenic-nuclide exposure dating was also revealing new information about the geomorphic processes that act to disturb and modify rock surfaces. Many subsequent exposure-dating studies showed the same phenomenon of increasing scatter with landform

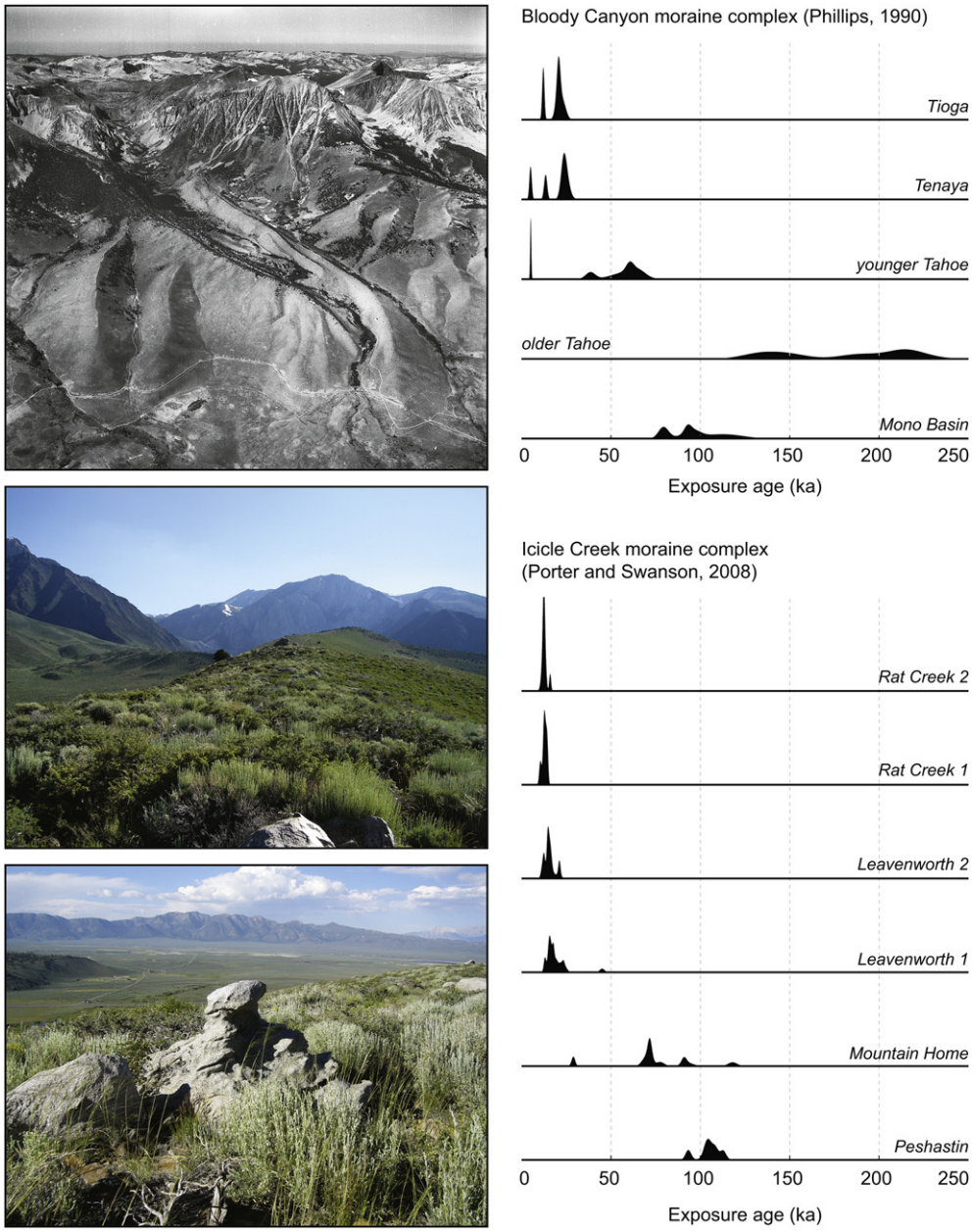


**Fig. 7.** Moraine disturbance and scatter in exposure-age data sets from alpine-glacial moraine sequences. Upper left, aerial view of the Bloody Canyon moraine complex in the eastern California Sierra Nevada (Phillips et al., 1990). Photo by Austin Post; courtesy of the Geophysical Institute, University of Alaska Fairbanks. Center left, ground-level view of a "Tahoe" moraine in the nearby Convict Canyon moraine sequence. The moraine was presumably sharp-crested at the time of emplacement and has been rounded by downslope soil creep. Lower left, a weathered boulder on this moraine. Evidently surface weathering affects the exposed portion of the boulder more intensely than the buried portion, so the tapered "hat" shape of the boulder indicates that both boulder surface weathering and moraine surface lowering have taken place since emplacement. Upper right, "camel plots" or summary probability diagrams (e.g., Lowell, 1995) for exposure ages from the Bloody Canyon moraines. Lower right, equivalent diagrams for exposure ages from the moraine sequence in the Icicle Creek Valley near Leavenworth, Washington, USA (Porter and Swanson, 2008). In both right-hand panels, moraines are arranged by stratigraphic age. Both data sets clearly show that older moraines have more outliers and greater overall scatter among exposure ages. The disagreement between stratigraphic age and exposure age for the oldest moraine in the Bloody Canyon data set indicates that all the boulders that were exposed at the time of moraine emplacement have been destroyed by weathering, and the boulders that were dated were most likely exposed at a later time by degradation of the moraine itself.

age; Fig. 7 shows an example, and Putkonen and Swanson (2003) demonstrated the phenomenon using a data set from nearly all other studies that were available at the time. These observations made it very clear that pristine glacial landforms are unusual rather than common, and that understanding postdepositional disturbance processes was important in determining the true age of any exposure-dated landform.

The current proliferation of exposure-dating studies, especially those on alpine-glacial moraine sequences, demonstrates several other important points about the issue of geologic scatter due to postdepositional disturbance. First, the geomorphic environment matters. As expected from the models of Hallet and Putkonen (1994), Putkonen and O'Neal (2006), and Putkonen et al. (2008) among others, postdepositional disturbance is most severe on sharp-crested alpine-glacial moraines that are emplaced as loosely consolidated boulder piles resting at the angle of repose (Fig. 9). These are most prevalent in steep, rapidly eroding mountain ranges, and the most extreme degrees of excess scatter in moraine

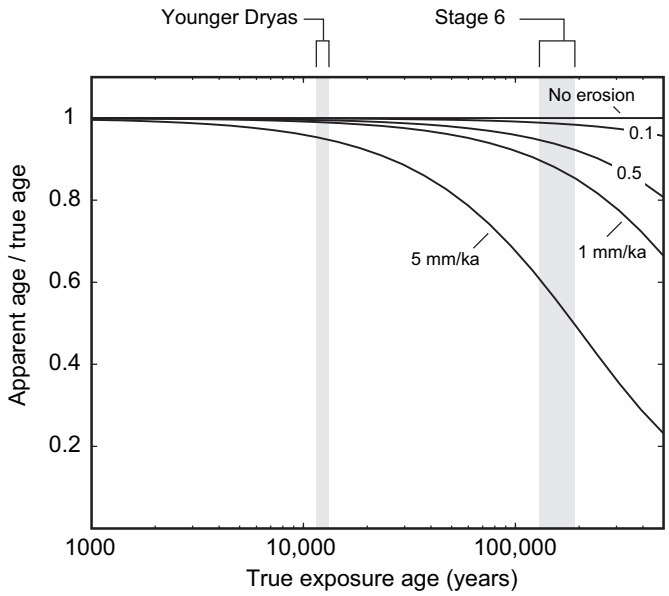


**Fig. 8.** Effect of rock surface erosion on apparent exposure ages for moraine boulders. The apparent exposure age is the exposure age computed from a surface cosmogenic-nuclide concentration under the assumption that the surface has not eroded. Because rock from the present surface was partially shielded from the cosmic-ray flux in the past by material that has since been eroded, the apparent exposure age of an eroded surface will always be less than its true exposure age. Typical surface erosion rates for crystalline rocks in temperate regions are 0.5–2.5 mm $ka^{-1}$. Erosion of this magnitude, if not accurately estimated and corrected for, would have a relatively minor effect on the inferred age of, for example, a Younger Dryas moraine. However, it would most likely preclude credible identification of a moraine deposited during the penultimate glacial maximum (marine oxygen isotope stage 6, ca 130–160 ka).

exposure ages yet documented occur at glaciers in the Himalaya (Scherler et al., 2010, and references therein) and the Alaska Range (Dortch et al., 2010). In contrast, moraine complexes deposited by continental ice sheets are commonly broad-crested and relatively flat, which reduces the importance of downslope creep in uncovering or disturbing erratic boulders. In addition, moraine complexes formed by continental ice are much larger than those formed by alpine glaciers, which makes it more likely that boulders can be found in stable landscape positions. Exposure-age data sets from continental ice sheet moraines that display little excess scatter are common (e.g., Clark et al., 2003; Rinterknecht et al., 2004; Balco and Schaefer, 2006; Fig. 10). The second point is that, in comparing exposure-dated alpine glacier chronologies to millennial-scale climate events, geologic uncertainty matters. A paper by Barrows et al. (2007) describing exposure ages from the Waiho Loop moraine of the Franz Josef Glacier in New Zealand, and a comment on this paper by Applegate et al. (2008) provide a clear example. Barrows et al. argued that postdepositional disturbance was not important and concluded that the moraine, previously thought to be an important example of a southern hemisphere Younger Dryas glacier advance, in fact postdated the Younger Dryas. Applegate et al. argued that postdepositional disturbance was important, and if it was properly taken into account the apparent exposure ages would be consistent with a Younger Dryas age for the moraine. This example as well as many other studies make it clear that correlation between exposure-dated glacial chronologies (particularly in geomorphically active mountain regions) and independently dated climate events at centennial or even millennial resolution is simply not possible without understanding and correcting for geologic scatter.

The preceding paragraphs focused on geologic scatter caused by postdepositional disturbance, but excess scatter of exposure ages for moraine boulders can also be caused by cosmogenic-nuclide inheritance. As discussed above, inheritance is common in

**Fig. 9.** Menagerie of postdepositional disturbance processes active on recently abandoned alpine-glacial moraines. Left panel, left lateral moraine of the Goodspeed Glacier, Antarctic Dry Valleys. The boulder is ~1.5 m long; the geologist in the background is well downslope. Moraine abandonment typically leaves boulders precariously balanced on angle-of-repose slopes. This one is unlikely to maintain its current position for an extended period of time. Center panel, ice-cored moraine adjacent to the Boydell Glacier, northern Antarctic Peninsula. Boulders are 1.5–2.5 m in diameter. This moraine consists of a thin layer of drift covering stagnant glacier ice (visible in foreground). Ice melts more slowly where it is shadowed by large boulders, leaving these examples perched on ice pedestals in improbable positions. As the ice core of the moraine melts – which may take thousands of years in polar climates – these boulders will periodically topple into new positions. Right panel, left lateral moraine of the Nisqually Glacier, Mt. Rainier, Washington, USA, that records the Little Ice Age advance of this glacier. The partially exposed boulder in the foreground is 1.5 m in diameter. Dry ravel, gullying, and slope retreat on the angle-of-repose slope at right will remove boulders from the present spine of the moraine and expose new ones.

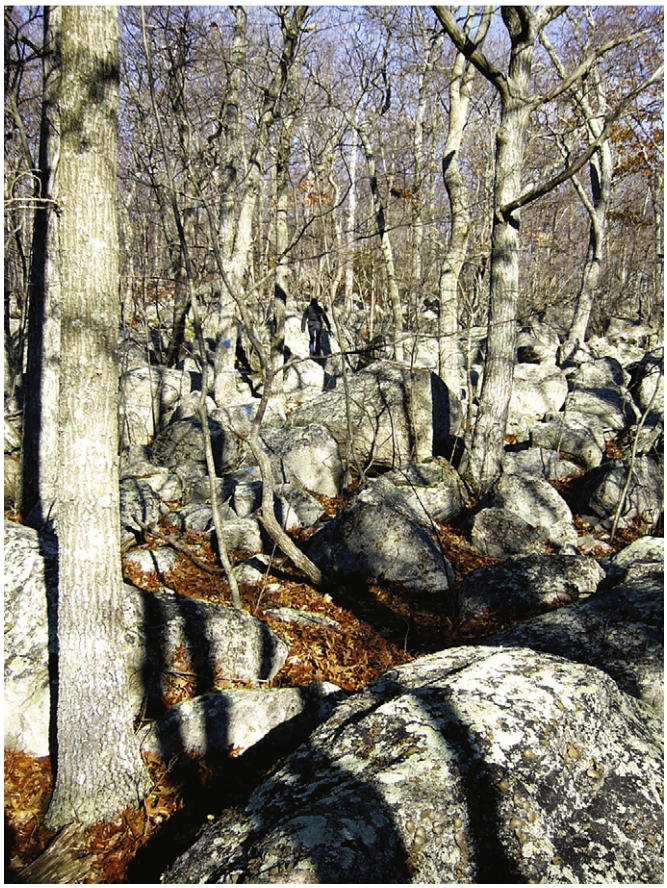

glaciated bedrock surfaces that were not sufficiently eroded by subglacial processes to remove the cosmogenic-nuclide inventory produced during older ice-free periods. Moraine boulders in alpine-glacial moraines could be emplaced with an inherited nuclide inventory in two ways: they could have been exposed for some time on an unglaciated summit above the ice surface and then been delivered to the glacier by rockfall rather than subglacial erosion, or they could have been deposited by a past glacier advance, exposed for a time, and then entrained and delivered to their present location by a later glacier advance. In contrast to postdepositional cover or surface erosion, which might be expected to have similar effects on many boulders on a moraine, most authors conceive of nuclide inheritance as a process that produces rare and easily recognizable outliers with wildly different exposure ages than the bulk of boulders on a moraine (e.g., Porter and Swanson, 2008). Putkonen and Swanson (2003) looked at this issue in a data set composed of nearly all exposure-dating studies available at the time, and found that only approximately 2% of dated moraine boulders could be characterized as obvious old outliers.

An unusual cause of geologic scatter, probably best placed in the category of inheritance, occurs in polar or high alpine regions where glaciers or ice sheets are frozen to their beds. It is well established that frozen-based glaciers can advance and retreat over delicate geomorphic features without disturbing them (e.g., Jonsson, 1983). In this situation, erratics deposited during one ice advance can remain undisturbed during one or many subsequent advances and retreats of cold-based ice. Thus, erratics deposited during previous ice-free periods can occur together with those deposited during the most recent deglaciation, and often it is impossible to tell the different generations of erratics apart in the field. Nearly all such examples are from Antarctic nunataks (e.g., Stone et al., 2003; Sugden et al., 2005; see Fig. 11). This particular situation has the advantages that it is clearly understood and binary: either the exposure age of an erratic reflects the most recent deglaciation, or it does not. Thus, these and subsequent researchers dealt with this issue by i) using geomorphic evidence for cover by cold-based ice to recognize when it is likely to be a problem, and ii) when this is the case, collecting and analysing enough erratics to clearly distinguish the age-elevation array reflecting the most recent deglaciation from the arrays that reflect past deglaciations.

### 6.2. Strategies for identifying and dealing with geologic scatter

There are two general strategies for identifying and dealing with geologic scatter: field observations and statistical methods. Many data sets exist that i) were collected by experienced glacial geologists who believed at the time that they were sampling pristine surfaces whose exposure age should correspond to the true emplacement age of a moraine, but ii) upon later analysis show a scatter of exposure ages exceeding that expected from measurement uncertainty alone. This observation suggests that neither strategy is adequate by itself, and the following discussion proceeds along both lines.

**Fig. 10.** Situations in which glacially transported boulders are unlikely to be disturbed by postdepositional processes. Upper panel, glacial erratics resting directly on ice-polished granite bedrock, Olmsted Point, Yosemite National Park, California. Because these boulders are firmly lodged in bedrock asperities rather than being supported by unconsolidated material, they are unlikely to move. Lower panel, recessional moraine deposited by the Laurentide Ice Sheet in eastern Connecticut. This moraine is located on flat ground and consists entirely of an interlocking, clast-supported pile of large boulders; finer material was removed by meltwater discharge (Goldsmith, 1982). It is unlikely that these boulders could be disturbed by creep or frost heave, and in fact exposure ages on seven boulders from this site agree within measurement uncertainty (Balco and Schaefer, 2006). At both these sites, of course, boulder exposure ages could be affected by surface weathering or snow cover.

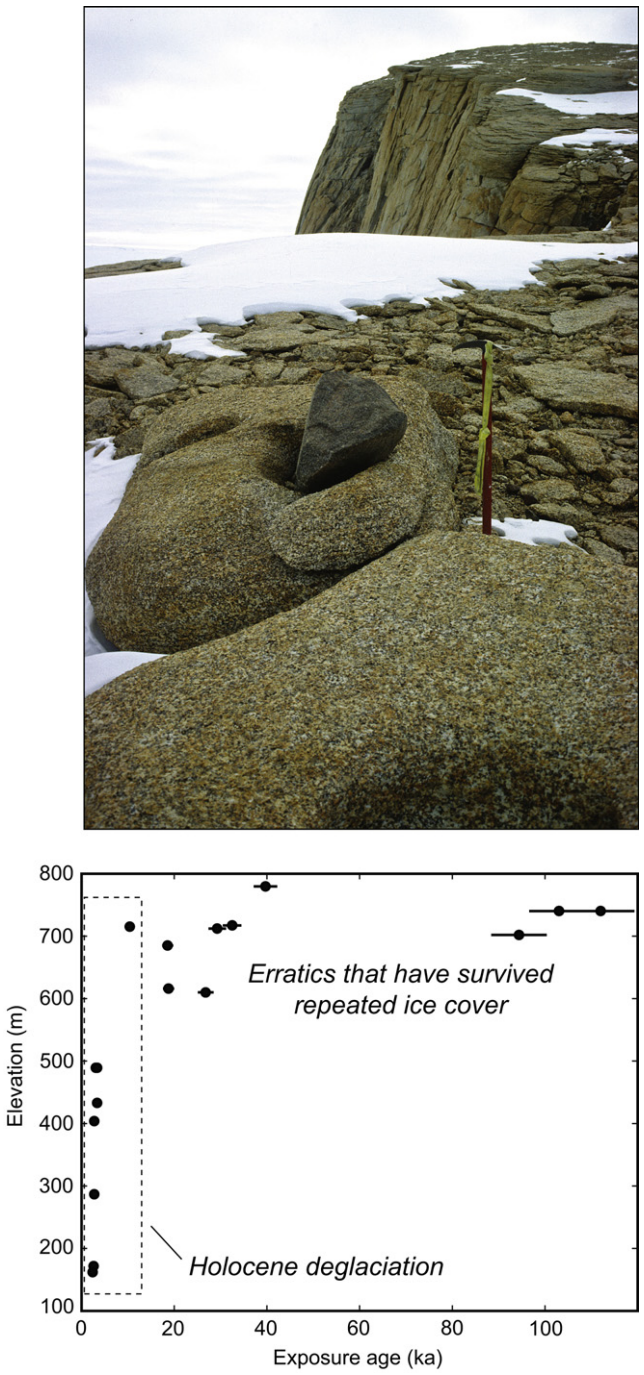


**Fig. 11.** Erratics emplaced during multiple successive ice-free periods and preserved together on Antarctic nunataks that are covered by cold-based ice during glacial maxima. The upper panel shows an erratic resting on cavernously weathered granite felsenmeer at high elevation on the Mt. Rea massif in the Ford Ranges of West Antarctica (77°03′ S, 145°33′ W). This relationship shows that the site was covered by cold-based ice that deposited erratics, but did not disturb delicate bedrock weathering features or displace loose slabs. The lower panel shows exposure ages on erratics from the Mt. Rea massif. Below 600 m elevation, only erratics deposited during the last, Holocene, ice retreat are present. Above this level, which presumably represents the highest elevation reached by the boundary between wet- and frozen-based ice during the Last Glacial Maximum, much older erratics that were deposited during previous ice-free periods are present. These data are from Stone et al. (2003) and Sugden et al. (2005).

The first important issue in interpreting a set of exposure ages from the same landform is to define what exactly "excess scatter" is, and detect whether or not it is present. The basic principle here is that scatter in exposure ages on a landform arises from two sources. First, measurement uncertainty, which typically amounts to several percent of the age, causes scatter even if all samples truly contain the same nuclide concentration. Second, geomorphic processes which affect the duration or intensity of cosmic-ray exposure of each sample differently cause the true nuclide concentration, and hence also the measured nuclide concentration, to differ among samples. The important difference between these two sources of scatter is that apparent scatter due to measurement uncertainty can be eliminated by averaging. If measurement errors are independent and normally distributed, as is true for typical analytical practices, then the mean of many measurements will yield a more accurate and more precise landform age than any one measurement. On the other hand, true scatter due to inheritance or postdepositional disturbance cannot be eliminated by averaging, because it is not likely that these processes will produce apparent exposure ages that are normally, or even symmetrically, distributed about the true landform age. Thus, the challenge in exposure dating is to differentiate data sets that are scattered due to measurement uncertainty (which can be averaged to produce a more accurate age) from those that are scattered due to geologic processes (which cannot).

#### 6.2.1. Statistical criteria

One set of strategies for dealing with this problem focuses on identifying data sets that scatter due to measurement uncertainty alone and/or discarding a small number of outliers to obtain such a data set. Some authors have simply declared that this is the case for their data set (e.g., Balco et al., 2002; Schaefer et al., 2002; Rinterknecht et al., 2004) and proceeded immediately to averaging. In general, however, strategies for detecting excess scatter have focused on statistical methods for determining whether the variance in a group of measurements is equal to that expected from the measurement uncertainty, the most commonly used of which is the reduced chi-squared statistic

$$\chi^2_R = \frac{1}{n-1}\sum_{i=1}^{n}\left[\frac{t_i - \bar{t}_i}{\sigma t_i}\right]^2 \quad (3)$$

where $t_i$ are the apparent exposure ages, $\bar{t}_i$ is their average, and $\sigma t_i$ are their uncertainties. If measurement uncertainty is the only source of scatter, the expected value of this statistic is $\sim 1$. Thus, several authors have observed that exposure-age data sets with reduced chi-squared values close to 1 could be averaged to yield a more accurate age for the landform (e.g., Barrows et al., 2002; Balco and Schaefer, 2006). This approach accords with basic statistical concepts and is likely a very effective method, but if strictly interpreted implies that any data set with an improbably high value of the reduced chi-squared or any similar statistic is uninterpretable and must be discarded. As is clear from the example in Fig. 12, the majority of exposure-age data sets from alpine glacier moraines has values much greater than 1, implying vanishingly low probability that measurement uncertainty is the only source of scatter. Because all of these data sets were generated at significant effort and expense, most researchers are unwilling to apply this approach strictly and discard them.

Some authors have used established statistical criteria (e.g., Chauvenet's criterion – Rinterknecht et al., 2006) to identify and discard outliers with low probability of belonging to the same population as the rest of the data set, thus yielding a subset of the data that can properly be averaged. This method is most likely appropriate in the case when only a minority of the data is outliers that reflect geologic scatter, but ineffective when most of the measurements, rather than only a few, are subject to geologic scatter. Finally, other authors (e.g., Balco et al., 2002; Clark et al., 2003) have omitted this step, simply asserted that certain of their measurements are outliers, and discarded them.

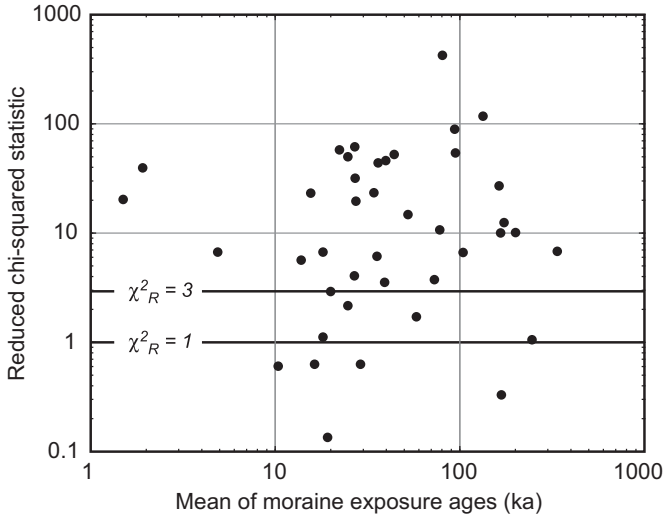


**Fig. 12.** Reduced chi-squared values for exposure ages on moraines in the Himalayas and Tibet, from Owen et al. (2002b, 2003a,c, 2005, 2006a,b, 2009). Only moraines with more than four exposure ages are shown. A reduced chi-squared value of 3, for a data set of six boulders, implies only a 1% chance that the observed scatter is due to measurement uncertainty alone. It is evident that strict adherence to this test, or any other statistical test for whether exposure ages from a particular moraine belong to a single population, would result in discarding the vast majority of these data sets. This highlights the importance of a better understanding of moraine disturbance processes in making sense of existing exposure-age chronologies in many mountain regions.

*6.2.2. Subsampling based on geomorphic arguments*

A second set of strategies can be described as subsampling from a data set on the basis of geomorphic arguments. Many authors have argued that exposure ages on glacial moraines are more likely to have a young bias due to moraine erosion and boulder weathering, and therefore that the true age of the moraine is best approximated by the oldest sample in a data set. Examples include Phillips et al. (1996) and Schaefer et al. (2006). Putkonen and Swanson (2003) considered this idea at length and provided guidelines for how to apply it in a consistent fashion to alpine-glacial moraines. On the other hand, Benson et al. (2004) argued that nuclide inheritance was more important than postdepositional erosion, and suggested that the youngest samples in their data sets best represented the true moraine ages. Finally, Benson et al. (2007) considered exposure ages from both recent and Lateglacial moraines at the same site as well as detailed observations of the sources, transport mechanisms, and condition of moraine boulders. They concluded that both inheritance and postdepositional disturbance were important, and arrived at the conclusion that the best estimate of the true moraine age was near the mean of the exposure ages. These strategies have the advantage that they are grounded in field observations, but two disadvantages. First, different, but presumably equally knowledgeable, geomorphologists can obtain wildly different age estimates for a single landform (for example, compare Brown et al., 2005 and Chevalier et al., 2005). Second, methods based on extreme estimators (i.e., the youngest or the oldest age) are absolutist in nature and fail completely if only one sample out of the entire data set fails to obey the geomorphic assumptions.

*6.2.3. Fitting predicted and observed exposure-age data sets*

A third strategy is based on the idea of matching modeled and observed distributions of exposure ages. The various geomorphic-argument-based estimators described above are all special cases of the idea that a physical model of the processes that deliver boulders to a moraine, and subsequently act to move, bury, exhume, or weather them, can be used to quantitatively predict the distribution of exposure ages on the moraine. This model must of necessity have the true emplacement age of the moraine as an input parameter. One can then find a moraine age that best fits the observations by optimizing the model parameters so that the predicted age distribution agrees best with the age distribution actually observed. Hallet and Putkonen (1994) and Putkonen and Swanson (2003) considered this idea in a general way, but did not carry out a formal model-fitting exercise. Recently Applegate et al. (2008, 2010), Applegate (2009) have applied this approach in a formal way by fitting predicted and observed exposure-age distributions to a variety of data sets from alpine-glacial moraines.

In my view this approach, specifically as applied by Applegate (see references above and Fig. 13), is a significant step forward in understanding and dealing with geologic scatter in exposure ages. It has the important advantages that i) it is based on field evidence in that field observations can be used to define and calibrate the geologic processes that are included in the model; ii) it relies on a fit to the entire data set, rather than relying on only one or a few of the data, so is more robust against low-probability events, iii) it captures the effect that the relationship between simple statistical descriptors of observed apparent exposure ages and the true exposure age of the moraine is a potentially complicated function of the geologic processes involved and their rates; and iv) the forward model results can be used to design a sampling program in such a way as to best constrain all the model parameters. Its key disadvantage is that the nature of comparing probability distributions, as well as the relatively large number of free parameters in the forward model, both necessitate a large number of measurements. Collecting large numbers of cosmogenic-nuclide exposure ages is time-consuming and expensive, and many researchers will not be persuaded that facilitating the application of this approach is worth doubling or tripling the expense of their study. However, this disadvantage is mitigated by the fact that many observations besides the exposure ages alone can be used to constrain the parameters of a moraine-degradation model. Such a model predicts many observables in addition to the exposure ages, including the topography of the moraine and the distribution, heights, and sizes of moraine boulders. Putkonen and O'Neal (2006) provided one example of this approach by relating a moraine-degradation model to the size and frequency of lichens on boulders (quantities that are much cheaper to measure than cosmogenic-nuclide exposure ages). It is very likely that expanding the model-data fitting exercise to include many field observations in addition to the exposure ages will increase confidence that the model accurately depicts the initial state of the moraine as well as the rates of the important processes, and in turn that a moraine emplacement age estimated from a model-data fit is accurate.

*6.2.4. Potential hybrid strategies*

Finally, there are many potential hybrid strategies, perhaps best described as statistical methods or highly simplified forward models informed by geomorphic principles, that have not yet been applied to the problem of identifying and accounting for geologic scatter. Two examples follow.

*6.2.4.1. Correlation of multiple measurements on the same samples.* As discussed above, many studies have used the reduced chi-squared statistic (or similar statistics) to argue that their data set is scattered due to measurement error only and can properly be averaged. One example appears in Balco et al. (2002), who stated that ten exposure ages from the Buzzards Bay moraine, a recessional moraine of the Laurentide Ice Sheet in eastern North America, were scattered at the level expected from measurement uncertainty, so the error-weighted mean of the data set was a more precise estimate of the true moraine age. In fact, this conclusion is not well supported by statistical measures. The reduced chi-squared value of this data

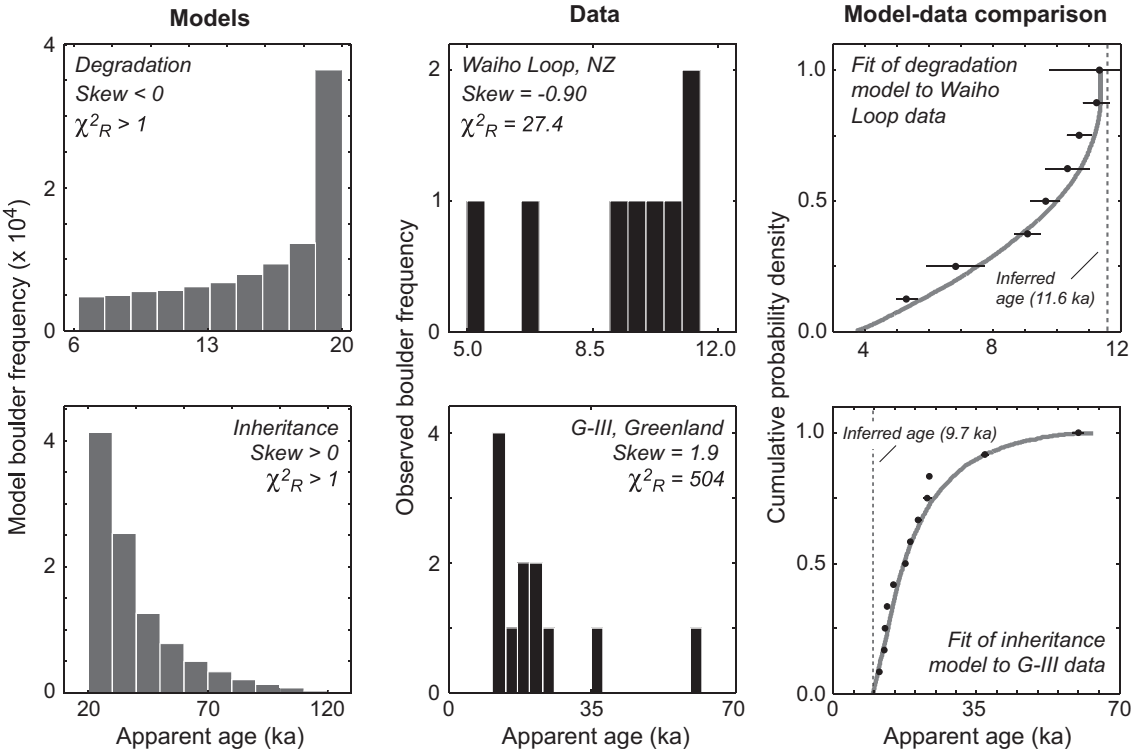


**Fig. 13.** Comparison of distributions of exposure ages on moraine boulders predicted by models of moraine degradation and inheritance (Applegate et al., 2010) to observed distributions. Upper panels show the fit of a model for moraine degradation to a set of $^{10}$Be exposure ages from the Waiho Loop moraine in New Zealand (Barrows et al., 2007). Lower panels show the fit of a model for boulder inheritance to a set of $^{10}$Be exposure ages from a Lateglacial moraine in Greenland (Kelly et al., 2008). The left-hand panels show histograms of boulder ages predicted by the model, and the center panels show histograms of observed exposure ages from these studies. Both models predict that observed exposure ages will scatter more than measurement uncertainty so will display high reduced chi-squared values. The moraine-degradation model predicts a negatively-skewed distribution of exposure ages, whereas the inheritance model predicts a positively-skewed distribution. The right-hand panels show the results of fitting modeled to observed distributions: the continuous curve is the cumulative probability distribution of exposure ages on moraine boulders predicted by the model and best-fit parameters, and the array of discrete ages is the observed cumulative probability distribution. The important parameter in the context of this discussion is the actual age the moraine was emplaced; best-fitting ages are shown on the right-hand panels. Details of models and model-data fitting appear in Applegate (2009) and Applegate et al. (2010). I thank Patrick Applegate for providing this figure.

set is 2.3, and the corresponding $p$-value — the probability that this value of the chi-squared statistic could arise by chance if measurement uncertainty is the only source of scatter — is 0.02. In other words, one can exclude the hypothesis that measurement uncertainty is the only source of scatter at 98% confidence. This is not very strong evidence against the presence of geologic scatter. These authors failed to consider a potentially stronger constraint provided by the fact that they made two exposure-age measurements — one by $^{10}$Be and one by $^{26}$Al — on each sample. This is important because measurements of $^{10}$Be and $^{26}$Al in a particular sample are independent. Thus, if we measure both nuclides in a set of samples that truly have identical exposure histories and therefore identical nuclide concentrations, exposure ages derived from $^{10}$Be and $^{26}$Al measurements will be uncorrelated. On the other hand, any process that causes variation in the exposure histories of the samples will affect both $^{26}$Al and $^{10}$Be concentrations together, and lead to a correlation between the two data sets.

This argument states that in a data set where the scatter is due to measurement uncertainty alone, $^{26}$Al and $^{10}$Be ages will be uncorrelated. If geologic scatter is present, they will be correlated. It can, in principle, be used both to evaluate whether geologic scatter is present and to determine which data should be excluded to yield a data set that is free of geologic scatter and can justifiably be averaged. One possible way to do this is as follows. First, determine whether the $^{26}$Al and $^{10}$Be measurements are correlated. A simple statistic for this purpose is the $p$-value of the linear correlation coefficient (e.g., $P_c$ of Bevington and Robinson, 1992), which is the probability that an observed linear correlation could arise by chance from uncorrelated data. Second, if the $^{26}$Al and $^{10}$Be measurements are correlated at high confidence by this measure, remove the sample that makes the largest contribution to the correlation. Third, repeat these steps until the remaining data display an acceptable $P_c$. The example below suggests that $Pc < 0.5$ is a reasonable threshold for acceptability, although it would be possible to derive appropriate values from many different lines of argument. This suggested procedure appears to have several advantages. It is based on a statistical measure that is sensitive to a fundamental difference in how measurement error and geologic scatter arise. It does not require presuppositions about the expected distribution of exposure ages or the geomorphic processes active at the site. It only allows a landform age to be computed if a significant fraction of the data set consists of samples that do represent the true landform age: if all of the ages are disturbed by postdepositional processes, it ought to be impossible to obtain an uncorrelated subset of the data. Finally, it provides a logically justifiable basis for subsampling the data set. On the other hand, there exist relatively few data sets where concentrations of multiple nuclides have been measured in the same samples, it is possible to create synthetic data sets that would cause this method to fail (for example, by imposing disequilibrium $^{26}$Al and $^{10}$Be concentrations), and it would not detect a hypothetical situation where all samples were disturbed equally by some process.

Applying this method to the Buzzards Bay data set (Fig. 14) reveals that the $^{26}$Al and $^{10}$Be measurements are correlated. In contrast to the assertion in the original paper, this shows that significant geologic scatter is present. Applying the pruning

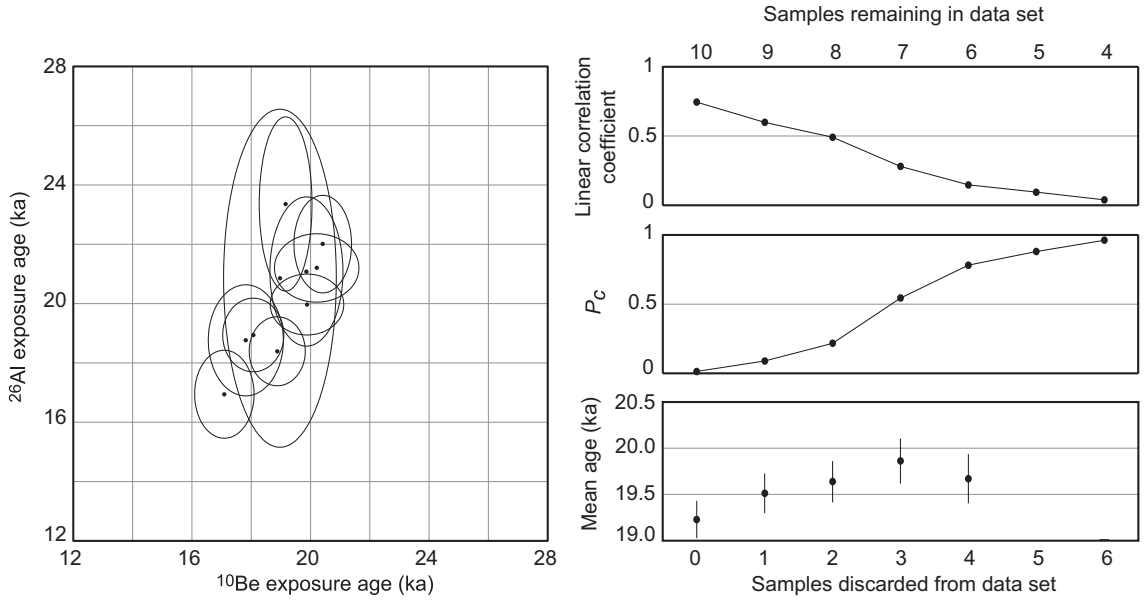


**Fig. 14.** Left panel, $^{10}$Be and $^{26}$Al exposure ages for ten boulders from the Buzzards Bay recessional moraine of the Laurentide Ice Sheet (Balco et al., 2002). The ellipses are 68% confidence regions. The two data sets are correlated. Right panels, results of "pruning" the data set by removing the samples that make the largest contribution to the correlation. After four samples are removed, the remaining data have an acceptably low correlation coefficient and *p*-value. The mean age from the resulting subsample of the data is 500 yr older than the mean of the entire data set.

algorithm above results in an uncorrelated data set after four measurements have been discarded. This implies that the mean of the remaining measurements is a better estimate for the true age of the moraine than the mean of the entire data set. In addition, it reveals that the samples that make the largest contribution to the correlation between $^{26}$Al and $^{10}$Be measurements are the youngest in the data set, which in turn suggests that the geologic process responsible for excess scatter is postdepositional cover or disturbance rather than nuclide inheritance. Looking back at the field notes for this study with this result in mind revealed that the four youngest exposure ages in the data set come from the four smallest boulders, which implicates soil or snow cover as a likely cause of geologic scatter. The point of this discussion is to show that this sort of a statistical analysis, combined with field observations, both: i) sheds light on the cause of excess scatter, and ii) provides a geomorphically and statistically justifiable strategy for subsampling the data set to yield a more accurate age for the moraine.

*6.2.4.2. Quantitative estimate of nuclide inheritance from exposure-ages on young samples.* The discussion so far in this section has highlighted the observation that the degree of excess scatter in an exposure-age data set commonly increases with moraine age, which implicates postdepositional disturbance as the likely cause. A set of exposure ages from Holocene to historic-age moraines in New Zealand collected by Schaefer et al. (2009) shows the opposite, in that excess scatter in these data decreases rapidly with moraine age (Fig. 15). This relationship cannot be explained by postdepositional disturbance. However, it can be explained if boulders are emplaced with small but significant inherited nuclide concentrations. In fact, one can predict it from the reasoning that i) the younger the moraine, the less postdepositional disturbance we expect, and ii) even if inherited nuclide concentrations are very small on average, as the age of a moraine approaches zero the inherited nuclide inventory will make up a greater and greater fraction of the total nuclide inventory. These authors recognized this basic concept, and used nuclide concentrations measured in two samples from a historically dated moraine to make an estimated inheritance correction. However, it is also possible to estimate the magnitude of nuclide inheritance from comparing the data set itself to a simple statistical model. The model consists of assuming that nuclide inheritance, here considered in units of years apparent exposure age, is random and uniformly distributed between 0 and $t_i$. If the true age of a moraine is $t_{\text{true}}$, then the measured age $t_m$ of a sample on that moraine is

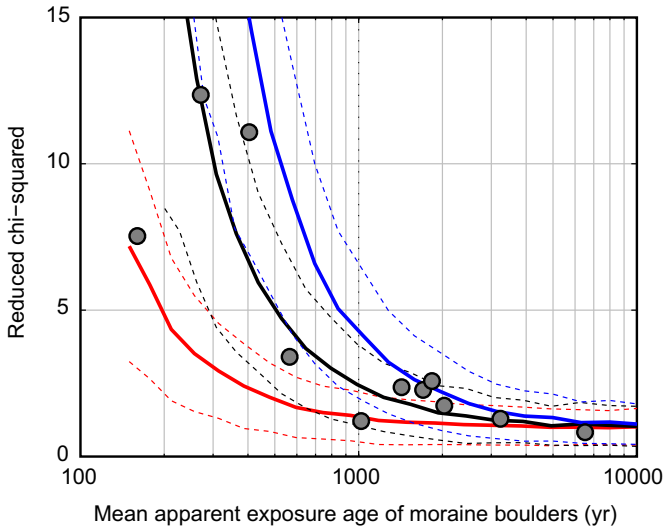


**Fig. 15.** Excess scatter in very young moraines explained by a nuclide-inheritance model. Circles show reduced chi-squared values for sets of exposure ages from 11 Holocene and recent alpine-glacial moraines in New Zealand (Schaefer et al., 2009). The observed inverse relationship between moraine age and excess scatter is unexpected if postdepositional disturbance processes are responsible for excess scatter. However, this relationship is expected if excess scatter is due to inherited cosmogenic-nuclide concentrations, which should be more evident as the nuclide concentration attributable to exposure after moraine emplacement becomes smaller. A simple uncertainty model reproduces this relationship and allows estimation of the magnitude of nuclide inheritance. Solid lines (and dashed 68% confidence bounds) show moraine age − excess scatter predicted by Equation (4), for maximum inheritance values $t_i$ (expressed as equivalent exposure age) of 100 yr (red), 200 yr (black), and 300 yr (blue). A uniform distribution of inheritance between 0 and 200 years explains the observations.

$$t_m = t_{\text{true}} + \varepsilon_m + \varepsilon_i \quad (4)$$

where $\varepsilon_m$ represents measurement uncertainty and is normally distributed with a mean of zero and a standard deviation of $\sigma_m$, and $\varepsilon_i$ represents nuclide inheritance and, as noted above, is uniformly distributed between 0 and $t_i$. Given a value for the maximum inheritance $t_i$ and a relationship between measured age $t_m$ and measurement uncertainty $\sigma_m$ (which is defined by the chemical preparation procedure and the AMS performance), one can predict the expected relationship between the age of a moraine and the scatter in exposure ages from that moraine using a Monte Carlo simulation (Fig. 15).

This model accurately reproduces the age–scatter relationship evident in the data set and has one free parameter ($t_i$). The best model-data match is obtained with $t_i$ near 200 yr, that is, a mean inheritance of 100 yr. This agrees with the inheritance inferred from the two historic samples (80 and 100 yr), but i) justifies applying the inheritance correction to the entire data set, and ii) permits a quantitative estimate of the total uncertainty in the moraine ages. The point here is again that combining data analysis, geomorphic principles, and a simple statistical model yields insight into the processes responsible for geologic scatter and provides a quantitative and physically justifiable means of accounting for it.

## 7. Production-rate scaling ambiguities and correlation with millennial-scale climate events

### 7.1. Examples of correlations rendered invalid or uncertain by production-rate scaling uncertainties

As discussed above in Section 5, the majority of studies that seek to correlate exposure-dated moraines with each other or with independently dated climate events at millennial time scales reach conclusions about these correlations that are not justifiable when uncertainties in the absolute value of nuclide production rates and in production-rate scaling are properly considered. Here I highlight several examples. Of course it is not possible to describe every one of these studies in an evenhanded fashion in the space available here, so in an effort to avoid favoritism I will begin with an example in which I proposed poorly justified correlations between exposure-dated moraines and millennial-scale climate events that were shown to be incorrect by more recent production-rate measurements.

Balco et al. (2002) exposure-dated moraine boulders from two prominent moraines of the Laurentide Ice Sheet in eastern North America: the terminal Martha's Vineyard moraine, and the recessional Buzzards Bay moraine. They computed the exposure ages according to the reference production rate and scaling scheme, current at the time, of Stone (2000), and found that the ages of the moraines were the same as the ages of i) increases in ice-rafted debris flux to the North Atlantic, and ii) prominent climate warmings evident in Greenland ice core records. They then concluded that the moraines were abandoned by ice margin retreat due to increases in ablation at these times (Fig. 16). Balco and Schaefer (2006) then exposure-dated moraine boulders from two additional recessional moraines to the north of (i.e., ice-proximal to and stratigraphically younger than) the Buzzards Bay moraine. Given the same production-rate calibration data set and scaling scheme used in the 2002 work, these moraines had apparent exposure ages that were younger than radiocarbon dates on post-glacial organic sediments stratigraphically overlying them. These exposure ages could not be correct, and Balco and Schaefer concluded that the most likely reason for this was an incorrect estimate of the $^{10}$Be production rate due to errors either in the

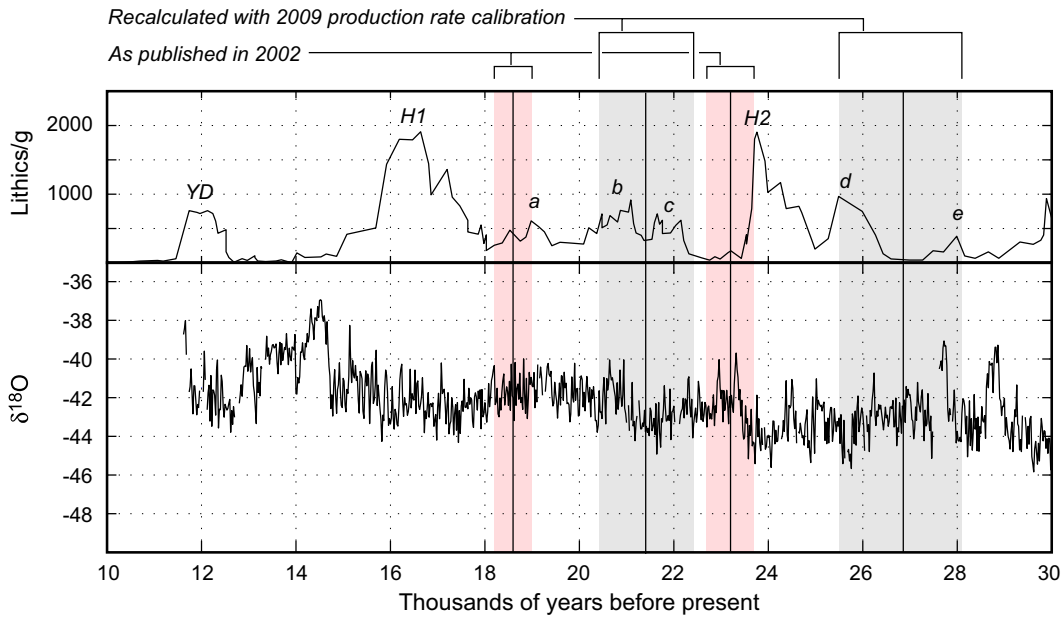


**Fig. 16.** Effect of errors in production-rate estimates on the correlation between terminal and recessional moraines of the Laurentide Ice Sheet at Martha's Vineyard, MA (Balco et al., 2002) and independently dated climate events. The upper panel shows ice-rafted debris concentrations in north Atlantic core V29-191 (Bond et al., 1997) and the lower panel shows the oxygen isotope record from the GISP2 ice core (Grootes and Stuiver, 1997) on the GICC05 time scale (Rasmussen et al., 2006). The vertical lines and shaded 1-standard-error uncertainty limits are weighted means of exposure ages from the Martha's Vineyard moraine (the terminal moraine; the older of the two) and the Buzzards Bay moraine (a recessional moraine; the younger of the two). Those shaded in red are the ages and uncertainties originally published in Balco et al. (2002), and those in gray reflect recalculation of the ages using the local production-rate calibration of Balco et al. (2009). The scaling scheme, selection of data to be averaged, and all assumptions about geologic scatter are unchanged from those in the original publication. Balco et al. (2002) originally proposed a correlation between the moraines and ice-rafted debris events H1 and "a" (red bands). The new production-rate calibration shows that although it is certainly possible that the moraines were coeval with one of the many other ice-rafted debris events, the originally proposed correlation is unlikely to be correct. This highlights the effect of systematic uncertainties in production-rate scaling on correlation between exposure-dated moraines and millennial-scale climate changes. In general, given moraines with age uncertainties of order 1000 years and millennial-scale climate changes, it is generally possible to propose a correlation between the two no matter whether they are truly temporally related or not.

scaling method or the production-rate calibration data. Balco et al. (2009) subsequently corrected this inconsistency by locating new production-rate calibration sites that were similar in location and age to the moraines whose age was in question. Production-rate measurements from these sites showed clearly that the production-rate estimates used in the previous studies were incorrect, and moraine exposure ages recalculated with this new local production-rate calibration no longer conflicted with the limiting radiocarbon ages. To summarize, the exposure ages, and in turn the correlations between moraines and climate events, in the 2002 paper were incorrect. Even without considering the likely disturbance of some of the moraine boulders by postdepositional processes as discussed in the previous section, the relationship of these moraines to climate events is unlikely to be as we originally claimed (Fig. 16). Finally, this example highlights the general observation that, given millennial-scale climate variability and exposure ages that may be subject to random or systematic uncertainties of order 1000 yr, it is nearly always possible to find apparent correlations (or anticorrelations) between the two even if there is no true causal or temporal relationship.

The example of the Martha's Vineyard and Buzzards Bay moraines is unusual because limiting radiocarbon dates showed unambiguously that a production-rate estimate was incorrect. In most cases, one chooses to exposure-date a moraine because there are no radiocarbon constraints on its age. For many moraines, therefore, different production-rate calibration data and scaling schemes simply predict different ages, and there is no way of confidently determining which is more accurate. The largest differences among scaling schemes currently in use occur at high elevation and low latitude, so this issue is most important for glacial records from the high tropical Andes and Himalayas. For example, Smith et al. (2005) exposure-dated boulders on LGM terminal moraines in the Peruvian Andes. Using the production-rate scaling scheme and calibration data set of Stone (2000), which was most commonly used at the time, they found that apparent exposure ages for these moraines were 25,000–35,000 years, and concluded that LGM glacier advances in the Andes significantly predated the maximum LGM extent of Northern Hemisphere ice sheets near 25,000 years ago. However, because their moraines are located at 4000 m elevation in the Andes, this conclusion is very sensitive to the choice of scaling scheme. Fig. 17 compares exposure ages, computed using the production-rate calibration data set of Balco et al. (2008) and five currently available scaling schemes, for the LGM moraines of Smith et al. with exposure ages from the terminal moraine of the Laurentide Ice Sheet at Martha's Vineyard (again from Balco et al., 2002 as discussed above). Smith et al. argued that LGM ice sheet advances in the tropical Andes significantly predated LGM advances of the Laurentide Ice Sheet. When these two exposure age data sets are compared using the scaling scheme that Smith et al. used, the comparison supports this argument. However, comparing the exposure ages using other scaling schemes fails to support it. In fact, some scaling schemes suggest that LGM advances in the Andes postdated retreat of the Laurentide Ice Sheet from its terminal moraine. There currently exists one production-rate calibration study (Farber et al., 2005) from the tropical Andes that could in principle help to establish which of these scaling schemes best predicts production rates at the Smith et al. sites, but the data in this study scatter more than expected from measurement uncertainty and the interpretation of the results depends on one's assumptions about postdepositional disturbance (Farber et al., 2005, also see discussion in Dunai, 2010). The important point here is that these comparisons do not show that the conclusions of Smith et al. are incorrect – it is certainly possible that their production-rate estimates will turn out to be accurate when more data are available – only that the divergence among a set of equally well justified production-rate estimates makes it impossible to know whether their conclusions are correct.

### 7.2. Strategies for mitigating production-rate uncertainties

Both examples described above were carried out and published before all the production-rate scaling schemes that are currently in use were available, at a time when the majority of exposure-dating studies employed the production-rate calibration data set and scaling method of Stone (2000). The subsequent development of new scaling schemes, as well as of relatively easy-to-use software (see discussion above) that allowed users to compute exposure ages according to a variety of different production-rate scaling schemes and calibration data, called attention to this issue. The effect of this emphasis has been that nearly all authors of current exposure-dating studies take the ambiguity caused by production-rate scaling uncertainties seriously, and are very conservative in correlating exposure-dated moraines with millennial-scale climate events (see, for example, Owen et al., 2008, 2009; Scherler et al., 2010). This approach certainly minimizes the likelihood of being wrong. However, because the overall goal of these studies *is* to establish the relationship between glacier change and climate change, it is not very satisfying. In this section I summarize research strategies designed to correct and not merely recognize the problem of production-rate estimation.

The best strategy would be to improve the accuracy of production-rate calibrations and scaling factors. Currently this is the subject of extensive research into i) the physical reasons for the divergence among currently available scaling schemes, ii) developing and improving scaling schemes based on physical principles rather than empirical fits to cosmic-ray flux measurements, iii) incorporating additional factors such as glacioisostatic rebound and changes in atmospheric pressure distribution into time-dependent scaling schemes; iv) locating additional production-rate calibration sites that span a wider range of age, elevation, and geomagnetic field characteristics than currently available sites, and v) improving the precision of the local production-rate measurements at the calibration sites. The details of this research are well beyond the scope of the present paper, but the important point is that production-rate estimates are very likely to become more accurate in future. However, this may take some time. In the meantime, there are two general approaches that are practical now.

The first approach echoes the discussion above in Section 5 in that it aims to design studies in such a way that the answers to the important questions are not dependent on scaling uncertainty. In that section, I highlighted examples of this approach that worked because only very coarse time resolution was required to answer the questions. However, several studies have used this idea to apply exposure-age data sets from glacial moraines to questions involving millennial-scale climate changes. For example, Schaefer et al. (2006) compared exposure ages from the innermost LGM moraines preserved at mid-latitude (ca 40–45°) mountain ranges in both hemispheres, and concluded that the termination of full-glacial conditions and onset of rapid deglaciation happened at the same time everywhere. This conclusion is only weakly sensitive to production-rate scaling uncertainties because all the moraines are at similar latitudes, at relatively high latitudes where sensitivity to production-rate variations due to magnetic field change is relatively unimportant, and at similar elevations. Thus production rates are similar at all sites, which minimizes the importance of scaling uncertainty. In addition, because all the moraines were dated by $^{10}$Be exposure ages, the absolute value of the $^{10}$Be production rate does not affect the time relationship between them. Of course, as correctly pointed out by these authors, the absolute value of the production rate does affect the relationship between the apparent exposure ages of these moraines and other independently dated climate events. A second example involves very young – historic and late Holocene – moraines in New Zealand dated by Schaefer

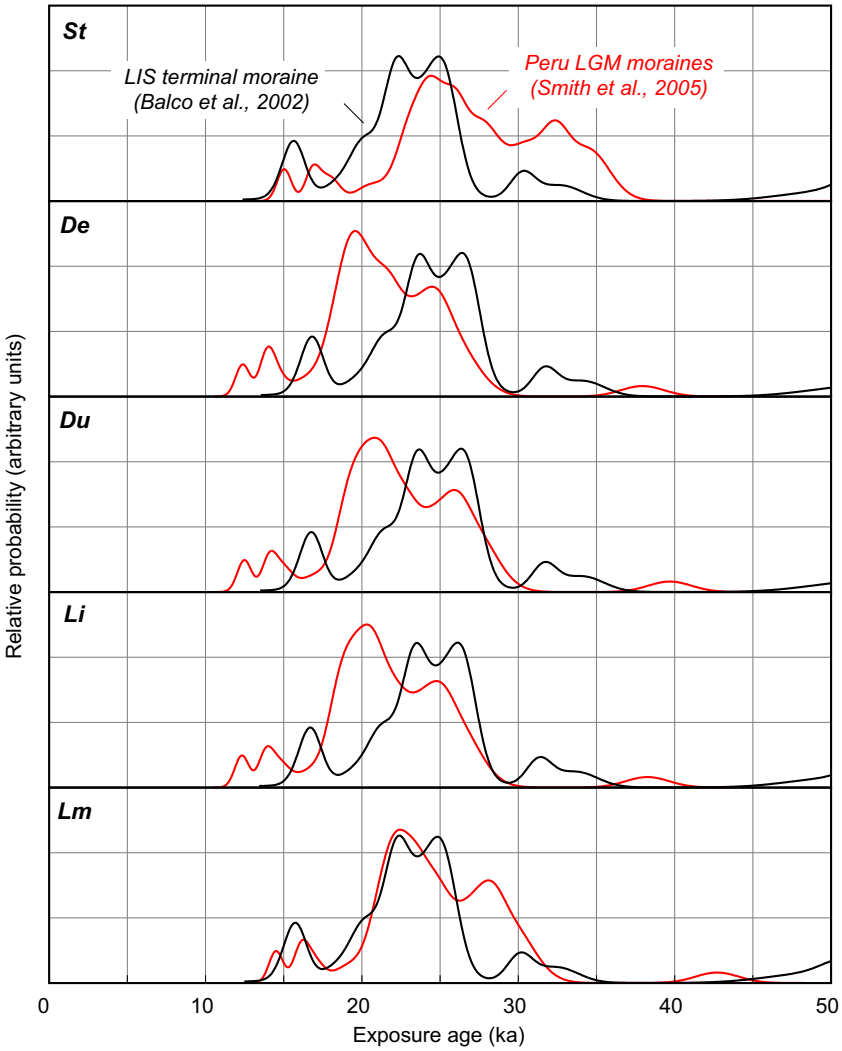


**Fig. 17.** Effect of production-rate scaling uncertainty on the conclusions of Smith et al. (2005) that mountain glaciers in the Peruvian Andes reached and began to retreat from their LGM terminal positions significantly earlier than northern hemisphere ice sheets. These show "camel plots" or summary probability diagrams (e.g., Lowell, 1995) for exposure ages of boulders on LGM terminal moraines of Peruvian mountain glaciers (in red; "Group C" moraines of Smith et al., 2005) and on the LGM terminal moraine of the Laurentide Ice Sheet in eastern North America (in black; Balco et al., 2002). In each panel, the exposure ages are computed using a different one of the five production-rate scaling schemes implemented in the online exposure-age calculators of Balco et al. (2008), and the two-letter scaling scheme designations follow those in that reference. The scaling scheme most similar to that originally used by Smith et al. (2005) (the 'St' scaling scheme shown in the top panel) yields results that support their conclusions that Peruvian glaciers retreated from their LGM terminal positions before northern hemisphere ice sheets. However, other scaling schemes lead to a different conclusion, that retreat from LGM moraines at both sites took place at the same time. This highlights the importance of systematic uncertainties in production-rate scaling schemes when exposure-dating moraines in regions where a large geographic extrapolation from production-rate calibration sites is required.

et al. (2009). The purpose of this study was to gain insight into millennial-scale Holocene climate changes by asking whether or not Holocene glacier advances in New Zealand occurred at the same time as those at various northern hemisphere sites, and these authors sought to do this by comparing $^{10}$Be exposure ages from the New Zealand moraines with radiocarbon-dated glacier chronologies from the other sites. Because scaling uncertainty in exposure ages stems from an uncertainty in the time-averaged production rate, it is manifested as an approximately constant relative uncertainty in exposure age. Thus, as exposure ages become younger, the production-rate uncertainty becomes smaller in absolute terms. The radiocarbon chronologies, from the Alps and British Columbia in particular, were in large part derived from trees and shrubs that grew at times when glaciers were smaller than present, remained in place during subsequent glacier overriding, and were re-exposed by recent glacier retreat. For late Holocene time, the radiocarbon-dated wood defines ice-free periods that are long compared to the uncertainty in the exposure ages, and this situation makes it possible to state with high confidence whether or not glaciers in New Zealand were larger than present at the time that the northern hemisphere glaciers were smaller than present.

The second approach is to minimize scaling uncertainties by obtaining production-rate calibration sites that are close in location and age to the unknown-age sites to be dated. The usual process of estimating production rates involves applying a particular scaling scheme to a set of globally distributed production-rate calibration data to obtain a reference production rate that, on average, best fits the entire global data set (Balco et al., 2008). However, as already discussed, existing scaling schemes cannot match the existing production-rate calibration data set within measurement uncertainty, which indicates that the results of this process will be incorrect for at least some locations and ages, and leads to the large production-rate uncertainties (ca 10%) that must be propagated into an exposure age calculated in this way. One can avoid this

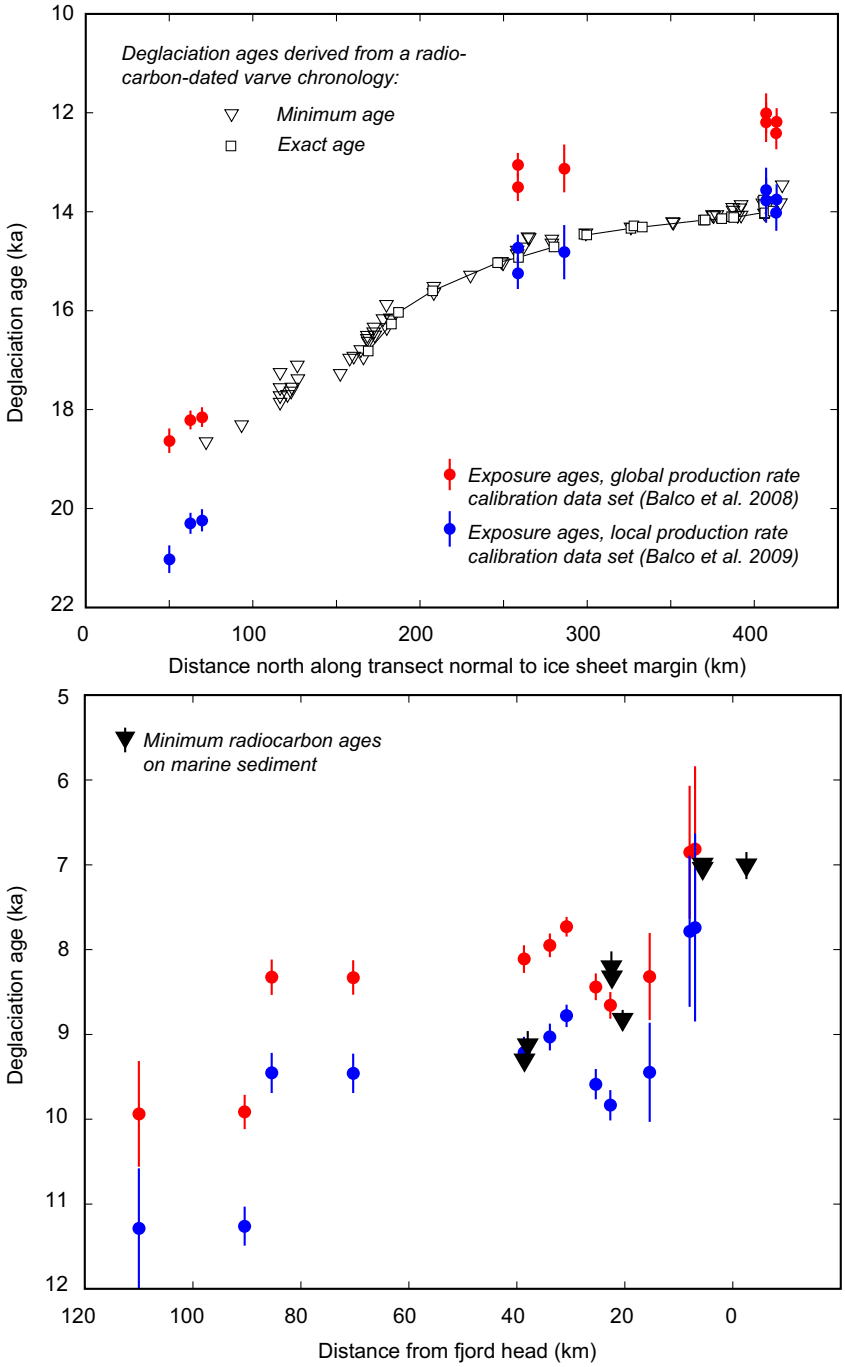


**Fig. 18.** Examples in which the use of a local production-rate calibration reconciles exposure ages and radiocarbon ages for deglaciation, thus increasing confidence in the accuracy of the exposure ages for the portion of the deglaciation chronology that cannot be radiocarbon dated. The upper panel shows an example from the northeastern U.S. (Balco et al., 2009) in which exposure ages on moraine boulders, when calculated with the global production-rate calibration data set of Balco et al. (2008), were younger than permitted by a radiocarbon-dated varve chronology. Computing exposure ages with local production-rate calibration measurements from northeastern North America instead reconciles the overlapping parts of the exposure age and radiocarbon chronologies, which in turn improves the accuracy of the exposure ages for moraines outside the radiocarbon chronology. The lower panel shows a similar example from Sam Ford Fjord on Baffin Island (Briner et al., 2009). Exposure ages calculated with the global production-rate calibration data set are younger than permitted by limiting radiocarbon ages on marine sediment. Using the production-rate calibration for northeastern North America corrects this inconsistency.

situation entirely by locating a production-rate calibration site at a similar location, and with similar age, to the sites one wishes to date. Then only a small scaling extrapolation is required and scaling uncertainty is minimized. Balco et al. (2009), as mentioned above, applied this approach to date moraines of the Laurentide Ice Sheet in the eastern U.S. Limiting radiocarbon ages showed that production-rate estimates derived from the global calibration data set with any scaling scheme yielded incorrect exposure ages for these moraines, so they identified other recessional moraines and ice-marginal features that had similar age and location to the moraines of unknown age, but had been independently dated. They measured $^{10}$Be concentrations on boulders from the independently dated landforms, used these to compute long-term average production rates, and then used these production rates to compute

exposure ages for the unknown-age moraines. This resulted in a chronology that agreed with all available radiocarbon age constraints (Fig. 18). In addition, the large production-rate uncertainty implied by trying to fit scaling schemes to the entire global calibration data set does not apply, so the precision of the ages with respect to independently dated records is significantly improved. In this example, formal external uncertainties on the exposure ages are ~6%. This equates to uncertainties of 600 yr on exposure ages of 10,000 yr, which is approaching adequate precision for correlation with Lateglacial climate events.

Putnam et al. (2010a,b) also used this strategy. They wished to date Lateglacial moraines in New Zealand, so located a nearby production-rate calibration site consisting of an early Holocene landslide deposit. The landslide overran a vegetated landscape, so radiocarbon dates on shrubs that were killed by the landslide accurately tell its age. It also has boulders on its surface whose $^{10}$Be concentration could be measured. As the $^{10}$Be concentrations from these boulders scatter at the level of measurement uncertainty, the apparent uncertainty on the long-term average $^{10}$Be production rate at this location is only a couple of percent. If taken at face value, this suggests that nearby Lateglacial and Holocene moraines can be absolutely dated at nearly the level of measurement precision for $^{10}$Be (again a couple of percent), which is precise enough for correlation with millennial-scale climate events.

To summarize, the fact that software tools now make it relatively easy to compute exposure ages with a wide range of scaling schemes and production-rate calibration data sets highlights the importance of scaling uncertainties. Currently these scaling uncertainties preclude correlation of exposure ages derived from the current global production-rate calibration data set with independently dated climate events at millennial scale. Longer-term research into production-rate systematics will eventually improve this situation for most ages and locations. At present, however, credibly relating exposure-dated glacier chronologies to millennial-scale Holocene and Lateglacial climate events requires either i) designing research questions so as to minimize the impact of scaling uncertainties on one's conclusions, or ii) finding local production-rate calibration sites near the sites of unknown age that one wishes to date.

## 8. Conclusions

Cosmogenic-nuclide dating of glacial landforms has made an outsize impact on the study of the chronology of glacier change because it filled an obvious need that had already been recognized by glacial geologists. Well before the method existed in any practical form, glacial geologists had widely adopted the general concept of "exposure dating" using a variety of exposure proxies, but the ideal proxy – one that was independent of local climate and environment, did not reach saturation quickly, and could be related from site to site based on physical principles – did not exist. If these geologists had been able to design an ideal solution to this problem, they would have arrived at something very similar to cosmogenic-nuclide exposure dating. Thus, it is no surprise that as soon as this method was developed, it was enthusiastically adopted by glacial geologists.

This method has resulted in major contributions to glacier chronology, the most significant of which are related to environments where no other dating method was possible. In my view the most important contribution of the method has been in Antarctica, where i) the environment makes radiocarbon dating of glacial deposits nearly impossible and, where possible, extremely difficult; ii) the LGM-to-present history of ice sheet change is of critical importance to understanding recent and future sea-level change, and iii) the important questions that have been answered by cosmogenic-nuclide exposure dating were broad enough that they are not sensitive to production-rate uncertainties. Other important contributions to glacier chronology have been in areas where dating of glacial deposits was likewise difficult or impossible before the advent of this method, most notably i) establishing the broad, and previously unknown, outlines of LGM-to-present glacier change in central Asia, and ii) making a start at an absolute chronology for pre-LGM mountain glaciations that could previously only be assigned relative ages. Finally, the unexpected discovery that many glaciated surfaces preserve cosmogenic-nuclide inventories from past as well as present ice-free periods provided a striking validation of theoretical work on subglacial processes.

The potential contributions that can be made in future with glacier chronologies based on exposure dating will stem from the steadily increasing precision of cosmogenic-nuclide measurements and from the sheer size of the data set of exposure-dated moraines. This data set is, in principle, large enough to be an important target data set for regional- and global-scale analyses of past climate dynamics (e.g., Rupper and Roe, 2008; Rupper et al., 2009). In fact, landforms that i) reflect past glacier change, and ii) can be exposure-dated, are commonly the only pre-instrumental records of climate change in mountain regions. The low detection limit of some cosmogenic nuclides means that the method can also be used to link historic and prehistoric records of glacier change. However, accurately relating exposure-dated glacier chronologies to climate events requires making significant progress in two areas: i) understanding and accounting for geologic processes that cause apparent exposure ages for glacial landforms to differ from their true emplacement age; and ii) minimizing systematic uncertainties in exposure ages contributed by production-rate calibration measurements and scaling factors. At present the number and distribution of glacial landforms that have been exposure-dated is certainly adequate to answer many important questions about past climate, but our understanding of production-rate uncertainties and geologic scatter is not. Thus, given the overall goal of incorporating exposure-dated glacier chronologies in paleoclimate syntheses, research focusing on these two issues will in the near future be more valuable than adding to the already very large data set of exposure-dated moraines.

## Acknowledgements

Patrick Applegate kindly provided Fig. 13. Bob Finkel, Brad Goodfellow, and Neil Glasser provided helpful reviews that improved the paper.

## References

Ackert, R., Barclay, D., Borns, H., Calkin, P., Kurz, M., Fastook, J., Steig, E., 1999. Measurements of past ice sheet elevations in interior West Antarctica. Science 286, 276–280.

Ackert, R., Singer, B., Guillou, H., Kaplan, M., Kurz, M., 2003. Long-term cosmogenic $^{3}$He production rates from $^{40}$Ar/$^{39}$Ar and K–Ar dated Patagonian lava flows at 47° S. Earth and Planetary Science Letters 210, 119–136.

Applegate, P., 2009. Estimating the ages of glacial landforms from the statistical distributions of cosmogenic exposure dates. Ph.D., Pennsylvania State University, State College, PA, USA.

Applegate, P., Lowell, T., Alley, R., 2008. Comment on absence of cooling in New Zealand and the adjacent ocean during the Younger Dryas chronozone. Science 320, 746.

Applegate, P., Urban, N., Laabs, B., Keller, K., Alley, R., 2010. Modeling the statistical distributions of cosmogenic exposure dates from moraines. Geoscientific Model Development 3, 293–307.

Balco, G., Schaefer, J., 2006. Cosmogenic-nuclide and varve chronologies for the deglaciation of southern New England. Quaternary Geochronology 1, 15–28.

Balco, G., Stone, J., Porter, S., Caffee, M., 2002. Cosmogenic-nuclide ages for New England coastal moraines, Martha's Vineyard and Cape Cod, Massachusetts, USA. Quaternary Science Reviews 21, 2127–2135.

Balco, G., Stone, J., Lifton, N., Dunai, T., 2008. A complete and easily accessible means of calculating surface exposure ages or erosion rates from $^{10}$Be and $^{26}$Al measurements. Quaternary Geochronology 3, 174–195.

Balco, G., Briner, J., Finkel, R., Rayburn, J., Ridge, J., Schaefer, J., 2009. Regional beryllium-10 production rate calibration for late-glacial northeastern North America. Quaternary Geochronology 4, 93–107.

Barrows, T., Stone, J., Fifield, L., Cresswell, R., 2002. The timing of the Last Glacial Maximum in Australia. Quaternary Science Reviews 21, 159–173.

Barrows, T., Lehman, S., Fifield, L., De Dekker, P., 2007. Absence of cooling in New Zealand and the adjacent ocean during the Younger Dryas chronozone. Science 318, 86–89.

Benson, L., Madole, R., Phillips, W., Landis, G., Thomas, T., Kubik, P., 2004. The probable importance of snow and sediment shielding on cosmogenic ages of north-central Colorado Pinedale and pre-Pinedale moraines. Quaternary Science Reviews 193, 193–206.

Benson, L., Madole, R., Kubik, P., McDonald, R., 2007. Surface-exposure ages of Front Range moraines that may have formed during the Younger Dryas, 8.2 ka, and Little Ice Age events. Quaternary Science Reviews 26, 1638–1649.

Bentley, M., Fogwill, C., Le Brocq, A., Hubbard, A., Sugden, D., Dunai, T., Freeman, S., 2010. Deglacial history of the West Antarctic Ice Sheet in the Weddell Sea Embayment: constraints on past ice volume change. Geology 38, 411–414.

Beschel, R., 1950. Flechten als Altersmasstab rezenter Moränen. Zeitschrift für Gletscherkunde und Glazialgeologie 1, 152–161.

Bevington, P.R., Robinson, D.K., 1992. Data Reduction and Error Analysis for the Physical Sciences. WCB McGraw-Hill.

Bierman, P., Turner, J., 1995. Be-10 and Al-26 evidence for exceptionally low rates of Australian bedrock erosion and the likely existence of pre-Pleistocene landscapes. Quaternary Research 44, 378–382.

Bierman, P., Gillespie, A., Caffee, M., 1995. Cosmogenic age-estimates for earthquake recurrence intervals and debris-flow fan deposition, Owens Valley, California. Science 270, 447–450.

Bierman, P., Marsella, K., Patterson, C., Davis, P., Caffee, M., 1999. Mid-Pleistocene cosmogenic minimum age limits for pre-Wisconsinan glacial surfaces in southwestern Minnesota and southern Baffin Island; a multiple-nuclide approach. Geomorphology 27, 25–39.

Blackwelder, E., 1931. Pleistocene glaciation in the Sierra Nevada and basin ranges. Geological Society of America Bulletin 42, 865–922.

Bockheim, J., Wilson, S., Denton, G., Andersen, B., Stuiver, M., 1989. Late Quaternary ice-surface fluctuations of Hatherton glacier, Transantarctic mountains. Quaternary Research 31, 229–254.

Bond, G., Showers, W., Cheseby, M., Lotti, R., Almasi, P., deMenocal, P., Priore, P., Cullen, H., Hajdas, I., Bonani, G., 1997. A pervasive millennial-scale cycle in North Atlantic Holocene and glacial climates. Science 278, 1257–1266.

Brigham-Grette, J., 1996. Geochronology of glacial deposits. In: Menzies, J. (Ed.), Past Glacial Environments, vol. 2. Butterworth-Heineman, Oxford, UK, Ch. 14, pp. 377–410.

Briner, J., 1998. Using inherited cosmogenic Cl-36 to constrain glacial erosion rates of the Cordilleran ice sheet. Geology 26, 3–6.

Briner, J., Kaufman, D., Werner, A., Caffee, M., Levy, L., Manley, W., Kaplan, M., Finkel, R., 2002. Glacier readvance during the late glacial (Younger Dryas?) in the Ahklun mountains, southwestern Alaska. Geology 30, 679–682.

Briner, J., Miller, G., Davis, P., Bierman, P., Caffee, M., 2003. Last Glacial Maximum ice sheet dynamics in Arctic Canada inferred from young erratics perched on ancient tors. Quaternary Science Reviews 22, 437–444.

Briner, J., Bini, A., Anderson, R., 2009. Rapid early Holocene retreat of a Laurentide outlet glacier through and Arctic fjord. Nature Geoscience 2, 496–499.

Brook, E., Kurz, M., 1993. Surface-exposure chronology using in situ cosmogenic $^{3}$He in Antarctic quartz sandstone boulders. Quaternary Research 39, 1–10.

Brown, E., Edmond, J., Raisbeck, G., Yiou, F., Kurz, M., Brook, E., 1991. Examination of surface exposure ages of Antarctic moraines using in situ produced $^{10}$Be and $^{26}$Al. Geochimica et Cosmochimica Acta 55, 2269–2284.

Brown, E., Molnar, P., Bourlés, D., 2005. Comment on "Slip-rate measurements on the Karakoram Fault may imply secular variations in fault motion". Science 309, 1326.

Bruno, L., Baur, H., Graf, T., Schlüchter, C., Signer, P., Wieler, R., 1997. Dating of Sirius group tillites in the Antarctic Dry Valleys with cosmogenic $^{3}$He and $^{21}$Ne. Earth and Planetary Science Letters 147, 37–54.

Cerling, T., Craig, H., 1994. Cosmogenic $^{3}$He production rates from 39°N to 46°N latitude, western USA and France. Geochimica et Cosmochimica Acta 58, 249–255.

Chevalier, M.-L., Ryerson, F., Tapponier, P., Finkel, R., Van Der Woerd, J., Haibing, L., Qing, L., 2005. Slip-rate measurements on the Karakoram Fault may imply secular variations in fault motion. Science 307, 411–414.

Clapp, E., Bierman, P., 1996. Cosmo-calibrate: a program for calculating cosmogenic exposure ages. Radiocarbon 38, 151–152.

Clark, D., Bierman, P., Larsen, P., 1995. Improving *in situ* cosmogenic chronometers. Quaternary Research 44, 367–377.

Clark, P., Brook, E., Raisbeck, G., Yiou, F., Clark, J., 2003. Cosmogenic $^{10}$Be ages of the Saglek moraines, Torngat mountains, Labrador. Geology 31, 617–620.

Clark, P., Dyke, A., Shakun, J., Carlson, A., Clark, J., Wohlfarth, B., Mitrovica, J., Hostetler, S., McCabe, A., 2009. The Last Glacial Maximum. Science 325, 710–714.

Denton, G., Sugden, D., Marchant, D., Hall, B., Wilch, T., 1993. East Antarctic Ice Sheet sensitivity to Pliocene climate change from a Dry Valleys perspective. Geografiska Annaler 75, 4.

Desilets, D., Zreda, M., 2001. On scaling cosmogenic nuclide production rates for altitude and latitude using cosmic ray measurements. Earth and Planetary Science Letters 193, 213–225.

Desilets, D., Zreda, M., 2003. Spatial and temporal distribution of secondary cosmic-ray nucleon intensities and applications to in-situ cosmogenic dating. Earth and Planetary Science Letters 206, 21–42.

Desilets, D., Zreda, M., Prabu, T., 2006. Extended scaling factors for in situ cosmogenic nuclides: new measurements at low latitude. Earth and Planetary Science Letters 246, 265–276.

Dortch, J., Owen, L., Caffee, M., Brease, P., 2010. Late Quaternary glaciation and equilibrium line altitude variations of the McKinley River region, central Alaska Range. Boreas 39, 233–246.

Douglass, D., Singer, B., Kaplan, M., Mickelson, D., Caffee, M., 2006. Cosmogenic nuclide surface exposure dating of boulders on last-glacial and late-glacial moraines, Lago Buenos Aires, Argentina: interpretive strategies and paleoclimate implications. Quaternary Geochronology 1, 43–58.

Dunai, T., 2000. Scaling factors for production rates of in situ produced cosmogenic nuclides: a critical reevaluation. Earth and Planetary Science Letters 176, 157–169.

Dunai, T., 2001. Influence of secular variation of the magnetic field on production rates of in situ produced cosmogenic nuclides. Earth and Planetary Science Letters 193, 197–212.

Dunai, T., 2010. Cosmogenic Nuclides: Principles, Concepts, and Applications in the Earth Surface Sciences. Cambridge University Press, Cambridge, UK.

Dunai, T., Stuart, F., 2010. Reporting of cosmogenic nuclide data for exposure age and erosion rate determinations. Quaternary Geochronology 4, 437–440.

Dunai, T., Wijbrans, J., 2000. Long-term cosmogenic $^{3}$He production rates (152 ka–1.35 Ma) from $^{40}$Ar/$^{39}$Ar dated basalt flows at 29° N latitude. Earth and Planetary Science Letters 176, 147–156.

Elmore, D., Phillips, F., 1987. Accelerator mass spectrometry for measurement of long-lived radioisotopes. Science 236, 543–550.

Emslie, S., Coats, L., Licht, K., 2007. A 45,000 yr record of Adélie penguins and climate change in the Ross Sea, Antarctica. Geology 35, 61–64.

Farber, D., Hancock, G., Finkel, R., Rodbell, D., 2005. The age and extent of tropical alpine glaciation in the Cordillera Blanca, Peru. Journal of Quaternary Science 20, 759–776.

Fink, D., McKelvey, B., Hannan, D., Newsome, D., 2000. Cold rocks, hot sands: in-situ cosmogenic applications in Australia at ANTARES. Nuclear Instruments and Methods in Physics Research Section B: Beam Interactions with Materials and Atoms 172, 838–846.

Frankel, K., Finkel, R., Owen, L., 2010. Terrestrial cosmogenic nuclide data reporting standards needed. Eos, Transactions, American Geophysical Union 91, 31–32.

Goldsmith, R., 1982. Recessional moraines and ice retreat in southeastern Connecticut. In: Late Wisconsinan Glaciation of New England: Proceedings of the Symposium. Kendall/Hunt, Dubuque, Iowa, pp. 61–76.

Gosse, J., Klein, J., 1996. Production rate of *in-situ* cosmogenic $^{10}$Be in quartz at high altitude and mid latitude. Radiocarbon 38, 154–155.

Gosse, J.C., Phillips, F.M., 2001. Terrestrial in situ cosmogenic nuclides: theory and application. Quaternary Science Reviews 20, 1475–1560.

Gosse, J.C., Evenson, E., Klein, J., Lawn, B., Middleton, R., 1995. Precise cosmogenic $^{10}$Be measurements in western North America: support for a global Younger Dryas cooling event. Geology 23, 877–880.

Grootes, P., Stuiver, M., 1997. Oxygen 18/16 variability in Greenland snow and ice with $10^{3}$ to $10^{5}$ year time resolution. Journal of Geophysical Research 102, 26455–26470.

Hall, B., Denton, G., 2000. Radiocarbon chronology of Ross Sea drift, eastern Taylor Valley, Antarctica: evidence for a grounded ice sheet in the Ross Sea at the Last Glacial Maximum. Geografiska Annaler 82A, 305–336.

Hall, B., Hoelzel, A., Baroni, C., Denton, G., Le Boeuf, B., Overturf, B., Topf, A., 2006. Holocene elephant seal distribution implies warmer than present climate in the Ross Sea. Proceedings of the National Academy of Sciences of the United States of America 103, 10213–10217.

Hallet, B., 1979. A theoretical model of glacial abrasion. Journal of Glaciology 23, 39–50.

Hallet, B., 1986. Glacial quarrying: a simple theoretical model. Annals of Glaciology 22, 1–8.

Hallet, B., Putkonen, J., 1994. Surface dating of dynamic landforms: young boulders on aging moraines. Science 265 (5174), 937–940.

Hunt, A., Larsen, J., Bierman, P., Petrucci, G., 2008. Investigation of factors that affect the sensitivity of accelerator mass spectrometry for cosmogenic $^{10}$Be and $^{26}$Al isotope analysis. Analytical Chemistry 80, 1656–1663.

Ivins, E., James, T., 2005. Antarctic glacial isostatic adjustment: a new assessment. Antarctic Science 17, 541–553.

Johnson, J., Bentley, M., Gohl, K., 2008. First exposure ages from the Amundsen Sea Embayment, West Antarctica: the late Quaternary context for recent thinning of Pine Island, Smith, and Pope glaciers. Geology 36, 223–226.

Jonsson, S., 1983. On the geomorphology and past glaciation of Storöya, Svalbard. Geografiska Annaler 65A, 1–17.

Kelly, M., Kubik, P., Von Blanckenburg, F., Schlüchter, C., 2004. Surface exposure dating of the Great Aletsch Glacier Egesen moraine system, western Swiss Alps, using the cosmogenic nuclide $^{10}$Be. Journal of Quaternary Science 19, 431–441.

Kelly, M., Ivy-Ochs, S., Kubik, P., von Blanckenburg, F., Schlüchter, C., 2006. Chronology of deglaciation based on Be-10 dates of glacial erosional features in the Grimsel Pass region, central Swiss Alps. Boreas 35, 634–643.

Kelly, M., Lowell, T., Hall, B., Schaefer, J., Finkel, R., Goehring, B., Alley, R., Denton, G., 2008. A $^{10}$Be chronology of Lateglacial and Holocene mountain glaciation in the Scoresby Sund region, east Greenland: implications for seasonality during Lateglacial time. Quaternary Science Reviews 27, 2273–2282.

Kubik, P., Christl, M., 2010. $^{10}$Be and $^{26}$Al measurements at the Zurich 6 MV tandem AMS facility. Nuclear Instruments and Methods in Physics Research Section B: Beam Interactions with Materials and Atoms 268, 880–883.

Kubik, P., Ivy-Ochs, S., Masarik, J., Frank, M., Schlüchter, C., 1998. $^{10}$Be and $^{26}$Al production rates deduced from an instantaneous event within the dendrocalibration curve, the landslide of Köfels, Ötz Valley, Austria. Earth and Planetary Science Letters 161, 231–241.

Kurz, M., Colodner, D., Trull, T., Moore, R., O'Brien, K., 1990. Cosmic ray exposure dating with in situ produced cosmogenic $^{3}$He: results from young Hawaiian lava flows. Earth and Planetary Science Letters 97, 177–189.

Lal, D., 1991. Cosmic ray labeling of erosion surfaces: in situ nuclide production rates and erosion models. Earth and Planetary Science Letters 104, 424–439.

Larsen, P., 1996. In-situ production rates of cosmogenic $^{10}$Be and $^{26}$Al over the past 21,500 years determined from the terminal moraine of the Laurentide Ice Sheet, north-central New Jersey. Ph.D. thesis, University of Vermont.

Lawrence, D., 1950. Estimating dates of recent glacier advances and recession rates by studying tree growth layers. American Geophysical Union Transactions 31, 243–248.

Licciardi, J., Kurz, M., Clark, P., Brook, E., 1999. Calibration of cosmogenic $^{3}$He production rates from Holocene lava flows in Oregon, USA, and effects of the Earth's magnetic field. Earth and Planetary Science Letters 172, 261–271.

Licciardi, J., Kurz, M., Curtice, J., 2006. Cosmogenic $^{3}$He production rates from Holocene lava flows in Iceland. Earth and Planetary Science Letters 246, 251–264.

Lifton, N., Bieber, J., Clem, J., Duldig, M., Evenson, P., Humble, J., Pyle, R., 2005. Addressing solar modulation and long-term uncertainties in scaling secondary cosmic rays for in situ cosmogenic nuclide applications. Earth and Planetary Science Letters 239, 140–161.

Lifton, N., Smart, D., Shea, M., 2008. Scaling time-integrated in situ cosmogenic nuclide production rates using a continuous geomagnetic model. Earth and Planetary Science Letters 268, 190–201.

Lowell, T., 1995. Application of radiocarbon age estimates to the dating of glacial sequences: an example from the Miami sublobe, Ohio, USA. Quaternary Science Reviews 14, 85–99.

Marchant, D., Denton, G., Swisher, C., Potter, N., 1996. Late Cenozoic Antarctic paleoclimate reconstructed from volcanic ashes in the Dry Valleys region of southern Victoria Land. Geological Society of America Bulletin 108, 181–194.

Marsella, K., 1998. Timing and extent of glaciation in the Pangnitung Fjord region, Baffin Island: determined using in situ produced cosmogenic Be-10 and Al-26. Master's thesis, University of Vermont.

Marsella, K., Bierman, P., Davis, P., Caffee, M., 2000. Cosmogenic Be-10 and Al-26 ages for the Last Glacial Maximum, eastern Baffin Island, arctic Canada. Geological Society of America Bulletin 112, 1296–1312.

Masarik, J., Reedy, R., 1995. Terrestrial cosmogenic-nuclide production systematics calculated from numerical simulations. Earth and Planetary Science Letters 136, 381–395.

Masarik, J., Frank, M., Schäfer, J., Wieler, R., 2001. Correction of in situ cosmogenic nuclide production rates for geomagnetic field intensity variations during the past 800,000 years. Geochimica et Cosmochimica Acta 65, 2995–3003.

Niedermann, S., 2002. Cosmic-ray-produced noble gases in terrestrial rocks: dating tools for surface processes. In: Porcelli, D., Ballentine, C., Wieler, R. (Eds.), Noble Gases in Geochemistry and Cosmochemistry. Reviews in Mineralogy and Geochemistry, vol. 47. Mineralogical Society of America, pp. 731–784.

Nishiizumi, K., Winterer, E., Kohl, C., Klein, J., Middleton, R., Lal, D., Arnold, J., 1989. Cosmic ray production rates of $^{26}$Al and $^{10}$Be in quartz from glacially polished rocks. Journal of Geophysical Research 94, 17907–17915.

Nishiizumi, K., Finkel, R., Klein, J., Kohl, C., 1996. Cosmogenic production of $^{7}$Be and $^{10}$Be in water targets. Journal of Geophysical Research 101 (B10), 22225–22232.

Nishiizumi, K., Imamura, M., Caffee, M., Southon, J., Finkel, R., McAnich, J., 2007. Absolute calibration of $^{10}$Be AMS standards. Nuclear Instruments and Methods in Physics Research Section B: Beam Interactions with Materials and Atoms 258, 403–413.

Owen, L., Finkel, R., Caffee, M., 2002a. A note on the extent of glaciation throughout the Himalaya during the global Last Glacial Maximum. Quaternary Research 21, 147–157.

Owen, L., Finkel, R., Caffee, M., Gualtieri, L., 2002b. Timing of multiple late Quaternary glaciations in the Hunza Valley, Karakoram Mountains, northern Pakistan: defined by cosmogenic radionuclide dating of moraines. Geological Society of America Bulletin 114, 593–604.

Owen, L., Finkel, R., Haizhou, M., Spencer, J., Derbyshire, E., Barnard, P., Caffee, M., 2003a. Timing and style of late Quaternary glaciation in northeastern Tibet. Geological Society of America Bulletin 115, 1356–1364.

Owen, L., Finkel, R., Minnich, R., Perez, A., 2003b. Extreme southwestern margin of late Quaternary glaciation in North America: timing and controls. Geology 31, 729–732.

Owen, L., Ma, H., Derbyshire, E., Spencer, J., Barnard, P., Nian, Z., Finkel, R., Caffee, M., 2003c. The timing and style of late Quaternary glaciation in the La Ji mountains, NE Tibet: evidence for restricted glaciation during the latter part of the last glacial. Zeitschrift für Geomorphologie Supplement 130, 263–276.

Owen, L., Finkel, R., Barnard, P., Ma, H., Asahi, K., Caffee, M., Derbyshire, E., 2005. Climatic and topographic controls on the style and timing of late Quaternary glaciation throughout Tibet and the Himalaya defined by $^{10}$Be cosmogenic radionuclide surface exposure dating. Quaternary Science Reviews 24, 1391–1411.

Owen, L., Caffee, M., Bovard, K., Finkel, R., Sharma, M., 2006a. Terrestrial cosmogenic nuclide surface exposure dating of the oldest glacial successions in the Himalayan orogen: Ladakh Range, northern India. Geological Society of America Bulletin 118, 383–392.

Owen, L., Finkel, R., Ma, H., Barnard, P., 2006b. Late Quaternary landscape evolution in the Kunlun Mountains and Qaidam basin, northern Tibet: a framework for examining the links between glaciation, lake level changes and alluvial fan formation. Quaternary International 154–155, 73–86.

Owen, L., Caffee, M., Finkel, R., Seong, Y., 2008. Quaternary glaciation of the Himalayan–Tibetan orogen. Journal of Quaternary Science 23, 513–531.

Owen, L., Robinson, R., Benn, D., Finkel, R., Davis, N., Yi, C., Putkonen, J., Li, D., Murray, A., 2009. Quaternary glaciation of Mount Everest. Quaternary Science Reviews 28, 1412–1433.

Phillips, F.M., Plummer, M., 1996. CHLOE: a program for interpreting in-situ cosmogenic nuclide data for surface exposure dating and erosion studies. Radiocarbon 38, 98.

Phillips, F.M., Leavy, B., Jannik, N., Elmore, D., Kubik, P., 1986. The accumulation of cosmogenic chlorine-36 in rocks: a method for surface exposure dating. Science 231, 41–43.

Phillips, F., Zreda, M., Smith, S., Elmore, D., Kubik, P., Sharma, P., 1990. Cosmogenic chlorine-36 chronology for glacial deposits at Bloody Canyon, eastern Sierra Nevada. Science 248, 1529–1532.

Phillips, F., Zreda, M., Benson, L., Plummer, M., Elmore, D., Sharma, P., 1996. Chronology for fluctuations in late Pleistocene Sierra Nevada glaciers and lakes. Science 274, 749–751.

Porter, S., Swanson, T., 2008. $^{36}$Cl dating of the classic Pleistocene glacial record in the northeastern Cascade Range, Washington. American Journal of Science 308, 130–166.

Putkonen, J., Swanson, T., 2003. Accuracy of cosmogenic ages for moraines. Quaternary Research 59 (2), 255–261.

Putkonen, J., Connolly, J., Orloff, T., 2008. Landscape evolution degrades the geologic signature of past glaciations. Geomorphology 97, 208–217.

Putkonen, J., O'Neal, M., 2006. Degradation of unconsolidated Quaternary landforms in the western North America. Geomorphology 75, 408–419.

Putnam, A., Denton, G., Schaefer, J., Barrell, D., Andersen, B., Finkel, R., Schwartz, R., Doughty, A., Kaplan, M., Schlüchter, C., 2010a. Glacier advance in southern middle-latitudes during the Antarctic Cold Reversal. Nature Geoscience 3, 700–704.

Putnam, A., Schaefer, J., Barrell, D., Vandergoes, M., Denton, G., Kaplan, M., Finkel, R., Schwartz, R., Goehring, B., Kelley, S., 2010b. In situ cosmogenic $^{10}$Be production-rate calibration from the Southern Alps, New Zealand. Quaternary Geochronology 5, 392–409.

Rasmussen, S., Andersen, K., Svensson, A., Steffensen, J., Vinther, B., Clausen, H., Siggaard-Andersen, M.-L., Johnsen, S., Larsen, L., Dahl-Jensen, D., Bigler, M., Röthlisberger, R., Fischer, H., Goto-Azuma, K., Hansson, M., Ruth, U., 2006. A new Greenland ice core chronology for the last glacial termination. Journal of Geophysical Research D: Atmospheres 111, D06102.

Rinterknecht, V., Clark, P., Raisbeck, G., Yiou, F., Brook, E., Tschudi, S., Lunkka, J.-P., 2004. Cosmogenic $^{10}$Be dating of the Salpausselkä I moraine in southwestern Finland. Quaternary Science Reviews 23, 2283–2289.

Rinterknecht, V., Clark, P., Raisbeck, G., Yiou, F., Bitinas, A., Brook, E., Marks, L., Zelčs, V., Lunkka, J.-P., Pavlovskaya, I., Piotrowski, J., Raukas, A., 2006. The last deglaciation of the southeastern sector of the Scandinavian Ice Sheet. Science 311, 1449–1452.

Rodbell, D., Smith, J., Mark, B., 2009. Glaciation in the Andes during the Lateglacial and Holocene. Quaternary Science Reviews 28, 2165–2212.

Rupper, S., Roe, G., 2008. Glacier changes and regional climate: a mass and energy balance approach. Journal of Climate 21, 5384–5401.

Rupper, S., Roe, G., Gillespie, A., 2009. Spatial patterns of Holocene glacier advance and retreat in Central Asia. Quaternary Research 72, 337–346.

Schäfer, J., Ivy-Ochs, S., Wieler, R., Leya, I., Baur, H., Denton, G., Schlüchter, C., 1999. Cosmogenic noble gas studies in the oldest landscape on Earth: surface exposure ages of the Dry Valleys, Antarctica. Earth and Planetary Science Letters 167, 215–226.

Schaefer, J., Tschudi, S., Zhao, Z., Wu, X., Ivy-Ochs, S., Wieler, R., Baur, H., Kubik, P., Schlüchter, C., 2002. The limited influence of glaciations in Tibet on global climate over the past 170,000 yr. Earth and Planetary Science Letters 194, 287–297.

Schaefer, J., Denton, G., Barrell, D., Ivy-Ochs, S., Kubik, P., Andersen, B., Phillips, F., Lowell, T., Schlüchter, C., 2006. Near-synchronous interhemispheric termination of the Last Glacial Maximum at mid-latitudes. Science 312, 1510–1513.

Schaefer, J., Denton, G., Kaplan, M., Putnam, A., Finkel, R., Barrell, D., Andersen, B., Schwartz, R., Mackintosh, A., Chinn, T., Schlüchter, C., 2009. High frequency glacier fluctuations in New Zealand differ from the northern signature. Science 324, 622–625.

Scherler, D., Bookhagen, B., Strecker, M., von Blanckenburg, F., Rood, D., 2010. Timing and extent of late Quaternary glaciation in the western Himalaya constrained by $^{10}$Be moraine dating in Garhwal, India. Quaternary Science Reviews 29, 815–831.

Schimmelpfennig, I., Benedetti, L., Fink, D., Pik, R., Blard, P.-H., Bourlés, D., Burnard, P., Williams, A., 2009. Sources of in-situ $^{36}$Cl in basaltic rocks. Implications for calibration of production rates. Quaternary Geochronology 4, 441–461.

Smith, J., Seltzer, G., Farber, D., Rodbell, D., Finkel, R., 2005. Early local Last Glacial Maximum in the tropical Andes. Science 308, 678–680.

Stone, J., 1998. A rapid fusion method for separation of beryllium-10 from soils and silicates. Geochimica et Cosmochimica Acta 62, 555–561.
Stone, J.O., 2000. Air pressure and cosmogenic isotope production. Journal of Geophysical Research 105 (B10), 23753–23759.
Stone, J., Ballantyne, C., Fifield, L., 1998. Exposure dating and validation of periglacial weathering limits, northwest Scotland. Geology 26, 587–590.
Stone, J., Balco, G., Sugden, D., Caffee, M., Sass III, L., Cowdery, S., Siddoway, C., 2003. Holocene deglaciation of Marie Byrd Land, West Antarctica. Science 299, 99–102.
Stroeven, A., Prentice, M., 1997. A case for Sirius group alpine glaciation at Mt. Fleming, south Victoria Land, Antarctica: a case against Pliocene East Antarctic Ice Sheet reduction. Geological Society of America Bulletin 109, 825–840.
Sugden, D., Balco, G., Cowdery, S., Stone, J., Sass III, L., 2005. Selective glacial erosion and weathering zones in the coastal mountains of Marie Byrd Land, Antarctica. Geomorphology 67, 317–334.
Todd, C., Stone, J., Conway, H., Hall, B., Bromley, G., 2010. Late Quaternary evolution of Reedy glacier, Antarctica. Quaternary Science Reviews 29, 1328–1341.
Tschudi, S., Schäfer, J., Zhao, Z., Wu, X., Ivy-Ochs, S., Kubik, P., Schlüchter, C., 2003. Glacial advances in Tibet during the Younger Dryas? Evidence from cosmogenic $^{10}$Be, $^{26}$Al, and $^{21}$Ne. Journal of Asian Earth Sciences 22, 301–306.
Vermeesch, P., 2007. CosmoCalc: an Excel add-in for cosmogenic nuclide calculations. Geochemistry, Geophysics, Geosystems 8 (Q08003).
Zreda, M., Phillips, F.M., Smith, S., Elmore, D., Kubik, P., Sharma, P., Dorn, R., 1991. Cosmogenic chlorine-36 production in terrestrial rocks. Earth and Planetary Science Letters 105, 94–109.
Zreda, M., England, J., Phillips, F., Elmore, D., Sharma, P., 1999. Unblocking of the Nares Strait by Greenland and Ellesmere ice-sheet retreat 10,000 years ago. Nature 398, 139–142.